Contrasted response to climate change of winter and spring grain legumes in southwestern France

Gatien Falconnier, Anthony Vermue, Etienne-Pascal Journet, Mathias Christina, Laurent Bedoussac, Eric Justes

Contrasted response to climate change of winter and spring grain legumes in southwestern France

Gatien N. Falconnier[1,2,3*], Anthony Vermue[3], Etienne-Pascal Journet[3,4], Laurent Bedoussac[5], Mathias Christina[1,2,7], Eric Justes[3,6]

[1] CIRAD, UPR AIDA, F-34398 Montpellier, France.

[2] AIDA, Univ Montpellier, CIRAD, Montpellier, France.

[3] Université de Toulouse, INRAE, UMR AGIR, F-31326, Castanet-Tolosan, France

[4] Université de Toulouse, INRAE, CNRS, LIPM, F-31326, Castanet-Tolosan, France

[5] Université de Toulouse, INRAE, ENSFEA, UMR AGIR, F-31326, Castanet-Tolosan, France

[6] PERSYST, Univ Montpellier, CIRAD, F-34398, Montpellier, France

[7] CIRAD, UPR AIDA, F-97743 Saint-Denis, Réunion, France.

* corresponding author: gatien.falconnier@cirad.fr

Abstract:

Climate change could undermine grain legumes ability to fix atmospheric nitrogen and their contribution to increase cropping systems sustainability. Pea (*Pisum sativum* L.) and faba bean (*Vicia faba* L.) are the two most widely grown grain legumes in Europe, yet the potential impact of climate change on their performances has not been quantified. We calibrated and evaluated the STICS soil-crop model for spring pea, winter pea and winter faba bean using experimental data from southwestern France and explored the effect of contrasting climate change scenarios. After calibration, STICS accurately simulated grain yield and amount of N_2 fixed for the experimental growing seasons. Assuming no change in crop management, mean and inter-annual variability of grain yield and fixed N_2 were assessed for historical (1995-2015), mid-

term (2020-2040) and long-term (2060-2080) periods in one location in southwestern France. We considered projections from three climate models and two Representative [CO_2] Pathways (RCP 4.5 and RCP 8.5). The climate models spanned a wide range of changes in temperature (+0.3 to +4.1 °C) and rainfall (-15% to +8%) depending on time horizon and RCP. Simulated grain yield increased over the long term in most scenarios (+1 to +25%), and spring pea tended to benefit less than winter pea and winter faba bean. Nevertheless, for the climate scenario with a decrease in rainfall and the strongest increase in temperature, simulated spring pea grain yield decreased by 28% while winter legumes yields were less affected (-14% for pea and no decrease for faba bean). Simulated changes in the amount of N_2 fixed followed the grain yield response. Temperature rise caused a shortening in crop cycle duration. Simulated temperature stress significantly increased for spring and winter pea in most climate change scenarios while winter faba bean was rather unaffected due to greater upper temperature thresholds. N_2 fixation of spring pea was reduced by above-optimal temperature during its vegetative growth in spring while N_2 fixation of winter legumes was enhanced by the increase in temperature during their vegetative growth in winter. Simulated drought stress only increased in the climate scenario predicting a decrease in rainfall. Overall, [CO_2] increase would allow offsetting negative effects of temperature and drought on grain yield and N_2 fixation, except for climate scenarios involving a decrease in rainfall and the strong increase in temperature. The contrasted simulated response of winter and spring grain legumes to climate change in southwestern France points to the opportunity to tap grain legume diversity and cultivar choice as an adaptation strategy.

Key-words: STICS, pea, faba bean, crop modelling

1. Introduction

Legumes are a key source of proteins for food and feed, and provide several ecosystem services (Watson et al., 2017). In particular, biological fixation of N_2 can improve nitrogen use efficiency in cropping systems and contribute to reduce mineral N-fertilizer application and greenhouse

gases emissions (Foyer et al., 2016). Pea (*Pisum sativum* L.) and faba bean (*Vicia faba* L.) are the two most widely grown winter and spring grain legumes in Europe, representing 0.47% and 0.36% of European utilized agricultural area, respectively. In 2018, pea and faba bean yield averaged 2.4 t/ha and 2.1 t/ha, respectively. France, Spain, Italy and United Kingdom and Germany are the top producing countries (http://ec.europa.eu/eurostat, last accessed 20/04/2020). Despite their advantages, legumes remain poorly adopted by farmers in Europe and their cultivated area has even been decreasing, notably due to high inter-seasonal yield variability (Cernay et al., 2015, Watson et al., 2017). Climate change is likely to affect grain legumes yield and N_2 fixing capacity thus hampering even more their capacity to be adopted by farmers and to deliver the expected benefits for cropping systems sustainability.

The response of grain legumes to climate change in Europe is expected to vary across seasons and regions, depending on the future changes in [CO_2], temperature, and precipitation. Temperature is expected to increase in North, Central and South Europe, multi-model climate projections indicating a warming of 1 to 5°C in 2081–2100 relatively to 1986–2005 depending on the Representative Concentration Pathway (RCP) considered. Annual rainfall is expected to increase in North and Central Europe (+1 to +12% depending on RCP) and to decrease in South Europe (-7 to -26% depending on RCP) (IPCC, 2013). Rise in temperature cause a shortening in crop cycle duration and thus decreases solar radiation interception by the crop (Craufurd and Wheeler, 2009). Glasshouse experiments have explored the impact of heat and drought stress on pea and faba bean growth. Heat stress, *i.e.* temperature above 30°C imposed during seed set and/or seed development compared with a baseline situation at 20-25°C, was found to (i) compromise flower, pollen grain and seed development (Bishop et al., 2016; Larmure and Munier-Jolain, 2019; Stanfield et al., 1966); (ii) decrease photosynthetic rate (Haldimann and Feller, 2005; McDonald and Paulsen, 1997); and (iii) decrease nitrogenase activity (Dart and Day, 1971). Water stress (*i.e.* plants grown in pots with soil let to dry near wilting point) reduces

74 root nodule activity and nitrogen-fixing potential (Sprent, 1972). Field experiments have
75 confirmed that heat and drougth stress can severely impact grain yield and N_2 fixation. For
76 example, Sadras et al. (2013) calculated a 0.31 $t.ha^{-1}$ loss in pea grain yield per 1 °C increase in
77 maximum temperature around flowering. Carranca et al. (1999) found a 40 and 70% decrease
78 in N_2 fixation of faba bean and pea related to a 45% decrease in seasonal rainfall. Elevated
79 [CO_2] on the other hand has a positive effect on net photosynthesis efficiency of these C_3
80 legumes thanks to a decrease in carbon loss through photorespiration (Wang et al., 2012).

81 How these environmental stresses will interact under plausible climate change scenarios, and
82 their potential impact on yield and N_2 fixation, have so far not been extensively quantified for
83 grain legumes such as pea and faba bean in temperate production areas. Quantifying the impact
84 of climate change and the factors driving yield change will be crucial for the design of relevant
85 adaptations and favor a push toward a greater adoption of grain legumes by farmers.

86 Crop models are relevant tools to quantify the impact of multiple stresses occurring with
87 different timing during crop growth (Asseng et al., 2015). STICS is a generic crop model that
88 is adapted to several grain legumes (Falconnier et al., 2019; Jégo et al., 2010) and accounts for
89 several temperature and water stresses on both grain formation and N_2 fixation. Though not
90 initially developed for climate change studies, it has been adapted to take into account climate
91 change issues, in particular the effect of elevated [CO_2] (Bergez et al., 2014).

92 The aim of this study was to assess the growth and N_2 fixation response of spring pea, winter
93 pea and winter faba bean to climate change in southwestern France, an area representative of
94 temperate Mediterranean environment. The studied area was characterized by summer droughts
95 and cool, wet winters, and has been identified as a climate change hot-spot (Giorgi, 2006). In
96 particular, the objectives were to: (i) calibrate and assess simulation accuracy of the STICS
97 soil/crop model under current climate; (ii) use the model to assess how these legume species
98 and cultivars would be affected by climate change; and (iii) identify the main abiotic factors

99 ([CO_2], temperature, rainfall) driving change in grain yield and N_2 fixation under future climate
100 in order to discuss relevant adaptation strategies.

101 ## 2. Methods

102 We calibrated the STICS model for pea (this study) and faba bean (Falconnier et al., 2019),
103 based on data from crop experiments with detailed monitoring of plant growth, as well as soil
104 water and nitrogen dynamics carried-out from 2002 to 2014 in southwestern France. Responses
105 to climate change of the two crops were then investigated using the parameterized model.

106 In what follows, we successively describe the study site and experimental data, the crop model
107 and its calibration, the historical and future climates, and the analysis of model simulations.

108 ### 2.1. Study site and experimental data

109 The study area in southwestern France falls into the temperate climatic group and belongs to
110 the north Mediterranean environmental zone (Peel et al., 2007). The typical cropping system of
111 the region is wheat–sunflower rotation. Diversified cropping systems include winter and spring
112 legumes (Plaza-Bonilla et al., 2017) usually sown in November-December and February-March
113 respectively and harvested between mid-June and mid-July. The experimental data was
114 collected in two sites: (i) National Research Institute for Agriculture, Food and Environment
115 (INRAE) in Auzeville (43°31'39"N 1°30'4"E, , 168 m above sea level), and (ii) “Centre
116 Régional de Recherche et d’Expérimentation en Agriculture Biologique de Midi-Pyrénées”
117 (CREAB-MP) in Auch (43°38'27"N 0°36'22"E, 134m above sea level). Collected data included:
118 (i) dates of emergence, end of juvenile phase, beginning of grain filling and maturity; (ii) in-
119 season variables (leaf area index, aboveground biomass, accumulated fixed N_2 and total
120 aboveground accumulated plant N, soil moisture content and soil mineral N content to
121 maximum rooting depth); and (iii) end of season variables (grain yield and total amount of N_2
122 fixed). Weather data was obtained from stations at the two sites. Measured variables included

daily maximum and minimum air temperatures (°C), precipitation (mm), global solar radiation (MJ m^{-2}), average wind speed (m s^{-1}) and relative humidity (%). Average rainfall over the growing season (November-July) for the experimental years was 528 mm and 542 mm at Auzeville and Auch, respectively. Average temperature over the growing season for the experimental years was 12.4 and 11.3 °C at Auzeville and Auch, respectively. Experimental plots were on deep clay-loamy soils in Auzeville with averaged maximum rooting depth of 135 cm, and on shallow clay loamy soils in Auch with averaged maximum rooting depth of 70 cm. Site, year, and management factors (cultivar, crop density, incorporation of a cover crop before planting and sowing date) defined 61 Site–Year–Management units (Table S1). The experiments were extensively described by Bedoussac and Justes (2010), Kammoun (2014) and Plaza-Bonilla et al. (2017).

2.2. Crop model

2.2.1. General overview of the STICS model

The soil–crop model STICS (Brisson et al., 2009, 2002, 1998) was chosen for its robustness (Coucheney et al., 2015) and ability to simulate grain legume growth and nitrogen fixation (Falconnier et al., 2019). STICS simulates daily carbon, water and nitrogen dynamics. Crops are defined by species parameters (*e.g.* potential radiation use efficiency), ecophysiological options (*e.g.* effect of photoperiod) and cultivar specific parameters (*e.g.* time to flowering). Required inputs are: (i) daily weather variables (minimum and maximum temperature, solar radiation, rainfall, wind speed and relative humidity, and [CO_2] for climate change simulations); (ii) permanent soil characteristics (*e.g.* field capacity and wilting point); and (iii) crop and soil management (*e.g.* sowing density, tillage). Crop temperature calculated from weather variables and photoperiod drive crop daily development. The model simulates: (i) daily root development to compute water and nitrogen uptake; and (ii) daily canopy establishment that drives

147 transpiration and light interception to produce crop biomass. Dry matter accumulation in grains
148 results from a dynamic harvest index that increases with time during the reproductive phase
149 (Amir and Sinclair, 1991). With regard to soil dynamics, net nitrogen mineralization from soil
150 organic matter and crop residues, nitrate leaching, ammonia and nitrous oxide gaseous
151 emissions are daily simulated as well as vertical water drainage when field capacity is exceeded.
152 STICS also simulates nitrogen acquisition and N_2 fixation of legumes. Nodule formation
153 depends on soil thermal time and sets potential fixation. The process equations of the soil-crop
154 system are based on a unique set of general parameters. An exhaustive description of inputs,
155 equations and default parameter values of the STICS model is given in Brisson et al. (2008)
156 and Bergez et al. (2014). Stress factors are computed daily and vary between 0 (maximum
157 stress) and 1 (no stress).

158 ### 2.2.2. Water and nitrogen stress

159 Water and nitrogen stresses can indirectly affect grain yield and N_2 fixation through plant
160 growth. The water stress factor – the ratio of actual to potential evapotranspiration – affects
161 radiation use efficiency and plant transpiration.

162 Actual N_2 fixation depends on: (i) shoot biomass growth rate (carbon limitation for N_2 fixation);
163 and (ii) water deficit defined as the proportion of soil layers in the nodulation area for which
164 moisture is above wilting point. The nitrate concentration in the nodulation layer also reduces
165 nitrogen fixation when it exceeds a maximal nitrate concentration threshold. Nitrogen stress
166 factor – the ratio of actual crop nitrogen concentration to critical crop nitrogen concentration
167 (Lemaire and Gastal, 1997) – affects Leaf Area Index increase, radiation use efficiency and
168 senescence.

169 ### 2.2.3. Effect of temperature and [CO_2] in the model

The model accounts for the effect of thermal stress on legume performance through three different processes: (i) reduction of radiation use efficiency and biomass growth; (ii) interruption of grain filling; and (iii) reduction of potential N_2 fixation.

For biomass growth (radiation use efficiency) and N_2 fixation, the model defines four cardinal temperatures: base (T_{min}), lower optimal (T_{opt1}), upper optimal (T_{opt2}) and maximum (T_{max}) temperatures. The model simulates a linearly increasing rate (thermal stress factor goes from 0 to 1) with daily average temperature from T_{min} to T_{opt1}, a stable maximum rate from T_{opt1} to T_{opt2} (stress factor of 1) and a linearly decreasing rate from T_{opt2} to T_{max} (stress factor goes from 1 to 0). For grain filling, the model defines only one daily maximal temperature above which grain filling stops (stress factor of 0 versus 1 otherwise).

An exponential function with a species–specific parameter (lower for C_4 than for C_3 crops) accounts for the effect of elevated atmospheric [CO_2] on radiation use efficiency (Bergez et al., 2014). This function allowed to account for the effect of elevated [CO2] on net photosynthesis of C_3 legumes species (Wang et al., 2012). STICS can account for the impact of elevated [CO_2] on transpiration efficiency with a specific option. However this option was not activated for this study, as increase in transpiration efficiency was not found to be a significant contributor to the response of C_3 legumes to elevated [CO_2] (Wang et al., 2012). A full description of the equations and parameters governing the stresses definition can be found in Brisson et al. (2008).

2.2.4. Parameterization and evaluation of the soil-crop model

35 Site–Year–Management units were already used for the calibration and evaluation of winter faba bean in a previous study: the dataset, measurement methods and calibration procedure are described in details in Falconnier et al. (2019). 26 Site–Year–Management units were added for the calibration and evaluation of winter and spring pea done in this study (Table S1), following

193 the procedure described in Falconnier et al. (2019) for faba bean. Below we summarize the
194 main steps of this calibration and evaluation procedure.

195 Soil analysis informed the soil input parameters required by the STICS model (Table S1).
196 Moisture at field capacity and wilting point were first obtained using pedo-transfer functions
197 (Saxton and Rawls, 2006) and also based on laboratory measurements on sieved soil for
198 Auzeville field capacity. Field capacity and wilting point were then adjusted for each trial by
199 using in situ soil water measurements at sowing, harvest and during crop cycle in order to
200 minimize the error between simulated and observed soil water content, as field measurements
201 have proven more reliable than laboratory measurements when simulating dynamic water
202 balance (Gijsman et al., 2002). Average maximum available water to maximum rooting depth,
203 *i.e.* soil water content at field capacity minus soil water content at wilting point, was higher in
204 Auzeville (178 mm) than in Auch (64 mm). Initial soil mineral nitrogen (nitrate and
205 ammonium) and water content were set based on the measurements for each Site–Year–
206 Management unit (Table S1).

207 The calibration procedure followed the three steps as described in Guillaume et al. (2011): (i) a
208 literature review to determine existing parameters; (ii) the direct measurement of parameters
209 using experimental data; and (iii) a mathematical parameter optimisation. The stepwise
210 optimisation focused successively on parameters related to crop development, leaves
211 development, root growth, shoot growth, N_2 fixation, N uptake for mineral-N and yield
212 formation. This optimisation was carried out with the OptimiSTICS software (Wallach et al.,
213 2011). The goodness-of-fit criterion – the average squared error between observed and
214 simulated value per Site–Year–Management units simulation – was minimised using a simplex
215 algorithm. We calibrated three separate plant files: spring pea, winter pea and winter faba bean.
216 Falconnier et al. (2019) give the details of the calibration for winter faba bean. The calibration
217 was performed on Site–Year–Management units covering a range of growing seasons,

management situations and two types of soil (40 Site–Year–Management units, Table S1). The units with growing season and/or management not used in calibration were used for model evaluation (21 Site–Year–Management units, Table S1).

Mean Bias Error (MBE) and its relative value (rMBE), Root Mean Square Error (RMSE) and its relative value (rRMSE), and Efficiency (EF) were calculated to quantify model performance with the optimised parameter set as follows:

$$MBE = \frac{1}{n}\sum_{i=1}^{n}(P_i - O_i) \quad (1)$$

$$rMBE = \frac{MBE}{\bar{O}} \times 100 \quad (2)$$

$$RMSE = \sqrt{\frac{1}{n}\sum_{i=1}^{n}(O_i - P_i)^2} \quad (3)$$

$$rRMSE = \frac{RMSE}{\bar{O}} \times 100 \quad (4)$$

$$EF = 1 - \frac{\sum_{i=1}^{n}(O_i - P_i)^2}{\sum_{i=1}^{n}(O_i - \bar{O})^2} \quad (5)$$

where O_i and P_i are the observed and simulated values for the i^{th} measurement, n is the number of observations and $\bar{O}$ is the mean of the observed values. The joint calculation of these four indicators allowed a detailed assessment of model accuracy.

2.3. Historical and future climates

The climate change impact study was carried-out for the site of Auzeville at INRAE station. The historical climate (1995-2015) data, belonging to INRAE, was obtained from the weather station at this site. Mean annual air temperature was 18.8 °C with daily temperature ranging from -8.8 to 40.4 °C. Mean annual precipitation was 654 mm ranging from 401 to 1000 mm. Mean annual cumulative global radiation was 5021 MJ m^{-2} ranging from 4373 to 5556 MJ m^{-2}. Average daily global radiation was 6, 17, 22 and 11 MJ m^{-2} in winter, spring, summer and fall, respectively.

240 For future climate, outputs from three Regional Circulating Models (RCM) available from the
241 European Coordinated Regional climate Downscaling Experiment (Euro-CORDEX,
242 http://www.euro-cordex.net/) (Jacob et al., 2014) and the Drias (http://www.drias-climat.fr/)
243 were selected. RCMs are high-resolution meteorological models that use boundary conditions
244 defined by coarse-resolution Global Circulation Models (GCMs) to produce downscaled
245 climate projections relevant for region-scale impact studies. Three GCM-RCM combinations
246 (further referred as "climate model") were used to span a range of changes in future temperature
247 and rainfall, namely (i) the Institute Pierre-Simon Laplace Climate Model with the weather and
248 research forecasting (ISPL_WRF) model, (ii) the Centre National de Recherches
249 Météorologiques Model and the Alladin model (CNRM_Alladin) and (iii) the Irish Centre for
250 High-end Computing EC-EARTH model and the HIRHAM5 model (EC-
251 EARTH_HIRHAM5).

252 Two greenhouse gas emission scenarios (Representative Concentration Pathways, RCPs) were
253 considered (Vuuren et al., 2011). In the high-emission RCP 8.5 scenario, [CO_2] reaches 1370
254 ppm by 2100 while in the intermediate mitigation RCP 4.5 scenario, [CO_2] stabilizes at around
255 650 ppm in 2100. Temperature, rainfall and daily solar radiation were bias-corrected using
256 quantile mapping (Themeßl et al., 2011). In quantile mapping, historical simulated values
257 (hindcasts) and observed values (historical weather data) are ordered by magnitude to obtain
258 Empirical Cumulative Distribution Functions (ECDF). The bias correction is an empirical
259 transfer function that allows to map hindcast ECDF onto observations ECDF. The correction
260 was performed with the R Package "qmap" (https://cran.r-
261 project.org/web/packages/qmap/qmap.pdf).

262 Changes in cumulative rainfall and average and maximum temperatures between future and
263 historical climates were calculated for the November-July period that corresponds to grain
264 legumes growing season in Auzeville. Climate models projections were used individually, as

we did not want to assess a mean change in temperature and rainfall, but rather explore a range of contrasting but plausible climate change scenarios.

2.4. Analysis of model simulations

Spring pea, winter pea and winter faba bean grain yield and fixed N_2 were simulated with the historical climate (1995-2015) and with future climate corresponding to the projections of the three climate models for RCP 4.5 and RCP 8.5. Two future 21-year periods were simulated, namely mid-term (2020-2040) and long-term (2060-2080). We assumed a similar crop management (sowing date, initial N and water) for simulation with historical and future climates. Winter faba bean was sown on November 20th, winter pea on December 10th and spring pea on February 4th. Sowing density was 30, 72, and 100 plants m^{-2} for winter faba bean, winter pea and spring pea, respectively. No cover crop incorporation prior to legume cultivation was considered.

For each 21-year periods (historical, mid-term and long-term), we computed a yield average that was then scaled by the historical yield simulated with the historical climate (1995-2015). The scaled yield (YS) for a given period *p* was computed as:

$$YS_p = \frac{Y_p}{Y_{historical}} \quad (6)$$

where Y_p is the 21-year simulated average yield for period *p* (mid-term or long-term) and $Y_{historical}$ is the 21-year simulated average yield under the historical climate (1995-2015).

Yield threshold for yield failure (YFT*)* was calculated as the 20th percentile of yield with historical climate (Guan et al., 2017) using the R function *quantile*. Probability of yield failure, – the probability to obtain a yield below YFT – was then calculated with empirical cumulative distribution functions as provided by the R function *ecdf*. For example, a probability of yield failure of 0.6 means that for 60% of the years over a 21-year future climate, simulated annual

288 crop yield was lower than the 20th percentile of the crop yield in the historical climate. Since
289 *ecdf* gave a discrete step function, the probability to obtain YFT with historical climate could
290 diverge marginally from 0.2. Following a similar procedure, scaled average N_2 fixation and
291 probability of N_2 fixation failure were computed.

292 Simulated heat and drought stress factors (see section 2.3.2 and 2.3.3) during vegetative phase
293 (sowing to beginning of grain filling) and during reproductive phase (beginning of grain filling
294 to maturity) were averaged per period. For each RCP and climate model, the effect of the period
295 on the simulated stress factors was tested using a linear analysis of variance (ANOVA) using a
296 probability of < 0.05. All analyses were performed with R 3.6.1 (R Development Core Team,
297 2019; http://www.R-project.org, last accessed 19/09/2019).

298 **3. Results**

299 **3.1. Crop parameterization and model evaluation**

300 Calibrated model parameters (Table S2) led to a satisfactory prediction of crop development
301 phenology (Figure S1). For beginning of grain filling, rRMSE was 3, 2 and 9% for winter faba
302 bean, winter pea and spring pea, respectively. For maturity, rRMSE was 7, 2 and 4% for winter
303 faba bean, winter pea and spring pea, respectively.

304 Grain yield, aboveground biomass, aboveground plant nitrogen and amount of fixed N_2 at
305 harvest were satisfactorily predicted, with rMBE ranging from 3 to 7% with calibration dataset
306 and -5 to 1% with evaluation dataset, and rRMSE ranging from 20 to 29% with calibration
307 dataset, and 24 to 26% with evaluation dataset (Figure 1).

308 The model was able to reproduce variation in total soil water content, both at specific dates
309 during the cropping season and at the end of season (Figures 2a, 2b). Variability in total soil
310 mineral nitrogen content at specific dates during cropping season and at the end of the season
311 was also well reproduced in calibration dataset (rRMSE = 33%) (Figure 2c). Variations in total

312 soil mineral nitrogen content in the evaluation dataset was less well reproduced (rRMSE = 49%)
313 (Figure 2d), but simulations were in the range of the observed low values.

314 These overall good performances on both plant and soil related variables point to the
315 consistency of the model in representing water and nitrogen supply by the soil and water and
316 nitrogen uptake by the crop.

317 **3.2. Future climates**

318 The climate projections spanned a wide range of change in temperatures and rainfall (Figure
319 3). The three selected climate models consistently predicted an increase in maximal and average
320 daily temperature during grain legumes growing season (November-July), likely to affect
321 differently winter and spring crops (Table 1 and Figure S2). Under RCP 4.5, increase in
322 maximal temperature (averaged across the growing season) ranged 0.3-1.1°C and 1.0-2.8°C for
323 mid-term and long-term projections respectively, depending on the climate model considered
324 (Table 1). Under RCP 8.5, increase in maximal temperature (averaged across the growing
325 season) ranged 0.5-1.5°C and 2.7-4.4°C for mid-term and long-term projections respectively,
326 depending on the climate model considered (Table 1).

327 Climate models diverged in their projections with regard to rainfall, CNRM-Alladin and EC-
328 EARTH_HIRHAM5 generally predicted an increase in rainfall, while ISPL_WRF generally
329 predicted a decrease (Table 2 and Figure S3). Under RCP 4.5, change in average growing
330 season rainfall ranged from -5 to +4% and from -8 to +8% for mid-term and long-term
331 projections, respectively, depending on the climate model considered (Table 2). Under RCP
332 8.5, change in average growing season rainfall ranged from -3 to +4% and from -15 to +3% for
333 mid-term and long-term projections, respectively, depending on the climate model considered
334 (Table 2).

335 **3.3. Impact of climate change on grain yield and amount of N_2 fixed**

For long-term projections, grain yield and amount of N_2 fixed increased in scenarios involving EC-EARTH_HIRAM5 and CNRM_Alladin climate models (Figures 4a, 4b). In most cases spring pea benefited less than winter pea and winter faba bean. For scenarios involving the ISPL_WRF climate model – the climate model that predicted the strongest increase in temperature and a decrease in rainfall – changes in yield were contrasted. With this climate model, under RCP 4.5 legume yield decreased and spring pea was more affected (28% yield decline) than winter pea and winter faba bean (-19% and +1% yield change, respectively) (Figure 4a). Under RCP 8.5, spring pea was also the most affected legume, with a 9% decrease in yield, while winter pea and winter faba bean benefited from climate change with a 15% and 39% increase in yield respectively.

Overall, when considering all climate change scenarios (Figures 4a, 4b), amount of N_2 fixed followed a pattern similar to the one observed for grain yield. However, amount of N_2 fixed tended to (i) benefit more from climate change (EC-EARTH_HIRAM5 and CNRM_Alladin climate models); or (ii) be less affected (ISPL_WRF climate model).

3.4. Impact of climate change on yield and N_2 fixation failure

For long-term projection, probability of grain yield failure remained relatively stable in scenarios involving EC-EARTH_HIRAM5 and CNRM_Alladin climate models (Figure 4c). Probability of failure for the amount of N_2 fixed showed contrasted response depending on legume crops (Figure 4d), with an increase for spring pea (except for EC-EARTH-HIRAM5; RCP 8.5) and a decrease for winter pea. For both yield and amount of N_2 fixed, the failure probability of spring pea was always higher than that of winter pea and winter faba bean.

For the scenarios involving the ISPL_WRF climate model, probability of yield failure would increase drastically for spring pea, reaching 64% and 43% for RCP 4.5 and RCP 8.5 scenarios respectively (Figure 4c). Probability of failure for amount of N_2 fixed would reach 57% for

360 spring pea for RCP 4.5, and decrease to 12% for RCP 8.5 (Figure 4d). Probably of failure for
361 yield and amount of N_2 fixed of winter faba bean and winter pea would be less affected (Figures
362 4c, 4d).

363 **3.5. Effect of temperature on crop growth and N_2 fixation**

364 **3.5.1. Effect on crop cycle duration**

365 The increase in temperature with future climate shortened crop cycle duration in all climate
366 change scenarios (Table 3). Depending on the projections and the climate change scenario, crop
367 cycle duration decreased from 0 to 29 days for spring pea, 0 to 28 days for winter pea and 0 to
368 35 days for winter faba bean. Crop cycle duration was significantly correlated ($P<0.001$) with
369 final grain yield: a decrease of one day in crop cycle duration corresponded to an average
370 decrease in grain yield of 30, 42 and 16 kg ha^{-1} for spring pea, winter pea and winter faba bean
371 respectively (Figure S4).

372 **3.5.2. Effect of thermal stress on radiation use efficiency, grain filling and N_2**
373 **fixation**

374 Heat stress for radiation use efficiency during the vegetative phase significantly increased in
375 mid and long-term projections for spring pea as shown by lower stress factor values in almost
376 all climate change scenario (Figure 5a and Table 4). On the contrary, thermal stress for radiation
377 use efficiency tended to decrease during the vegetative phase for winter faba bean.

378 Heat stress on radiation use efficiency during reproductive phase (Figure 5b) and heat stress on
379 grain filling (Figure 5c) increased for spring pea and winter pea in mid and long-term
380 projections in half of climate change scenarios. No increase in these stresses was observed for
381 winter faba bean (Figures 5b, 5c and Table 4).

382 For winter pea and winter faba bean, thermal stress for N_2 fixation usually significantly
383 decreased during the vegetative phase that occurred mainly in winter where temperature are
384 usually sub-optimal while it tended to increase for spring pea, as its vegetative phase occurs in
385 spring when temperature are already optimal (Figure 6a and Table 4). During reproductive
386 phase, heat stress for N_2 fixation remained mainly unaffected under the EC-EARTH-HIRAM5
387 and CNRM_Alladin projections and increased from 0 to 9% in the ISPL_WRF projection
388 (Figure 6b, Table 4).

389 **3.6. Effect of drought on crop growth and N_2 fixation**

390 There was no significant change in drought stress for biomass growth during the vegetative
391 period with EC-EARTH_HIRAM5 and CNRM_Alladin climate models (Figure 7a and Table
392 4). On the contrary, drought stress for biomass growth during reproductive phase significantly
393 increased in the climate change scenario with ISPL_WRF model for winter pea (Figure 7a and
394 Table 4), but was not different for spring pea and winter faba bean. With this climate change
395 scenario, drought stress on N_2 fixation increased significantly during reproductive phase for all
396 grain legumes (Figure 7b and Table 4).

397 **4. Discussion**

398 *4.1 Impact of climate change on grain legume functioning and yield formation*

399 Grain yield and amount of N_2 fixed increased in climate change scenarios involving moderate
400 temperature rise and no change in rainfall over the long term (*i.e.* with CNRM Alladin and EC-
401 EARTH_HIRAM5 climate models): grain yield increased by 1% to 25%, and amount of N_2
402 fixed by 8% to 34% depending on RCP and climate models. Our simulations show that the
403 effect of the increase in [CO_2] offsets the negative effects of heat stress on crop growth and N_2
404 fixation (see section 3.5 and 3.6). Pea and faba bean are C_3 species for which elevated [CO_2]
405 increases net photosynthesis (Ainsworth and Rogers, 2007). Such increase has been quantified

406 in Free Air CO_2 Enrichment (FACE) experiments in Australia where pea yield increased by
407 26% with [CO_2] at 550 ppm compared with current [CO_2] at 390 ppm (Bourgault et al., 2016).
408 In a similar FACE experiment in Australia, faba bean grain yield increased by 59% and amount
409 of N_2 fixed by 60% with elevated [CO_2] under well-watered conditions (Parvin et al., 2019). N_2
410 fixation benefits from elevated [CO_2], as the greater carbon supply often translates into
411 increased nodule biomass and stimulates N_2 fixation (Rogers et al., 2009).

412 Projection of ISPL_WRF climate model under RCP 4.5 was the most constraining climate
413 change scenario with strong temperature increase and rainfall reduction. In this scenario, [CO_2]
414 increase could not offset temperature and drought stress on grain yield and N_2 fixation: grain
415 yield decreased by 1% to 27% and amount of N_2 fixed by 0% to 13%. The FACE experiments
416 in Australia supports such simulation outcome, where [CO_2] increase (550 ppm) could not
417 offset the detrimental impact on yield of a 3-days heat wave on lentil (Bourgault et al., 2018).
418 Yield penalties with rising temperature are also supported by glasshouse experiments: (i) pea
419 yield decreased by 54% with an increase in day-night temperature from 20-15 to 30-25 °C
420 (McDonald and Paulsen, 1997); and (ii) faba bean yield declined by 24% after an increase in
421 day-night temperature for five days during anthesis (18-10 to 34-26 °C) (Bishop et al., 2016).
422 Such yield penalties were attributed to flower abortion, reduced grain filling duration and also
423 reduced seed weight (Bishop et al., 2016; McDonald and Paulsen, 1997). Reduced grain filling
424 duration and reduced seed weight due to heat stress on grain filling can be accounted for by
425 STICS: our diagnosis (see section 3.5) showed that reduced crop cycle duration (-6 days per
426 1°C temperature increase on average across RCPs, climate models and crops) and increased
427 heat stress occurred in the different climate change scenarios. Flower abortion is not explicitly
428 taken into account in the STICS model. However, if biomass growth is reduced during a short
429 period before the start of grain filling – by heat stress for example – it can affect the simulated
430 number of grains (Falconnier et al., 2019). We diagnosed a significant increase in simulated

heat stress on radiation use efficiency that causes a reduction in net photosynthesis. This result is in line with experimental findings on the impact of heat on photosynthesis of other grain legumes like lentil (Bourgault et al., 2018) and kidney bean (*Phaseolus vulgaris* L.) (Prasad et al., 2002).

Drought also can strongly affect yield and N_2 fixation, thus offsetting the beneficial effect of [CO_2] increase. Under current Mediterranean climate with mean annual rainfall of 320 mm, faba bean grain yield was 56% smaller in rainfed treatments with moderate water stress compared with full irrigation treatments (Karrou and Oweis, 2012). In southern Portugal with average seasonal rainfall of 520 mm, amount of N_2 fixed by faba bean and pea decreased by 40 and 70%, respectively, when seasonal rainfall decreased by 45% (Carranca et al., 1999).

Overall, the amount of N_2 fixed was less affected or benefited more from climate change than grain yield. This could be because temperature thresholds for N_2 fixation were higher than temperature thresholds for radiation use efficiency and grain filling, leading to lower heat stress on N_2 fixation than on radiation use efficiency. Maximum temperatures were set according to literature (Table S2), *i.e.* 40 and 35 °C for N_2 fixation of faba bean and pea, respectively, and 34°C and 30°C for radiation use efficiency of faba bean and pea, respectively. Consequently, the simulated contribution of synthetically fixed N_2 to total plant nitrogen increased by three percent (across crops, RCP and climate models) in future scenarios compared with historical climate.

The relatively large number of published experimental studies on the impact of elevated [CO_2], heat and drought on grain legumes contrasts with the paucity of crop modelling studies dealing with climate impact on grain legumes. Modelling studies on the impact of climate on crops in Europe focused mainly on cereals like maize and wheat (Webber et al., 2018). To our knowledge, there is only one published modelling study exploring the impact of climate change on cool-season grain legumes in temperate environments (Ravasi et al., 2020). In line with one

456 of the climate change scenario of our study, the simulations of Ravasi et al. (2020) indicated
457 that the increase in [CO_2] could not offset the negative impact of temperature and drought stress
458 on spring pea in Northern Italy. Impact of climate change on grain legumes was also
459 investigated with crop models in tropical environment, on peanut (Faye et al., 2018) and on
460 chickpea (Mohammed et al., 2017). In line with our study, these simulations pointed to slight
461 increases in yield of grain legumes with climate change thanks to the effect of [CO_2] increase
462 on plant growth. However, these studies did not investigate the impact of climate change on N_2
463 fixation.

464 *4.2 Contrasted responses to climate change between cultivars and species*

465 In our simulations, spring pea tended: (i) to benefit less from climate change when the effect of
466 [CO_2] increase offsets heat and drought stress; or (ii) to be more affected when [CO_2] could not
467 offset heat and drought stress compared with winter pea and winter faba bean. Spring pea
468 vegetative phase occurred in spring when temperatures are already high (Figure S2). Therefore,
469 STICS simulated an increase in heat stress for radiation use efficiency in long-term projections
470 in almost all climate change scenarios. On the contrary, winter pea vegetative phase occurred
471 in winter when temperatures are low (Figure S2) and an increase in heat stress for radiation use
472 efficiency only occurred in the scenarios with the strongest increase in temperature. Even in
473 these latter case of high increase in temperature, no increase in heat stress was simulated for
474 winter faba bean, due to greater threshold temperatures for photosynthesis (24-34 °C for faba
475 bean versus 20-30 °C for winter and spring pea) (Table S2). Similarly, thermal stress on N_2
476 fixation increased for spring pea because its vegetative growth occurred in spring when
477 temperatures were already optimal with historical climate. Conversely, it decreased for winter
478 pea and winter faba bean since their vegetative growth occurred in winter where temperatures
479 were sub-optimal with historical climate. Secondly, grain filling started later for spring pea than
480 for winter pea and winter faba bean (*i.e.* three days after winter pea and thirteen days after

winter faba bean on average across climate change scenarios). As a result, when heat stress on grain filling occurred, it was greater for spring pea than for the winter legumes (see section 3.3). In the scenarios with a decrease in rainfall, drought stress on spring pea did not change significantly, but yield decreased drastically, indicating that heat stress still prevailed in this case. Possibly, the heat stress constrained plant growth, thus reducing transpiration and the impact of the reduction in water availability (*e.g.* Affholder, 1997).

Earlier development, heat stress avoidance and thus greater yield potential of winter pea and winter faba bean over spring pea and spring faba bean were reported under current climate in central Europe (Neugschwandtner et al., 2019). For cereal crops, the better adaptation of winter barley over spring barley was also reported with simulations of the impact of climate change using a statistical model (Gammans et al., 2017).

4.3 Uncertainties in crop simulation

Crop models are increasingly used for climate change impact studies. Uncertainty in crop model simulation can arise from improper calibration (Wallach et al., 2019), model structure or climate predictions uncertainty (Tao et al., 2018).

If not calibrated against multiple in-season variables such as soil water content, plant nitrogen content or Leaf Area Index, soil-crop models run the risk of accurately simulating grain yield without accurately simulating growth dynamics. This can undermine their relevance for climate change studies (Challinor et al., 2014; Martre et al., 2015). Our calibration procedure involved the assessment of simulation accuracy for multiple in-season variables (soil water, soil nitrogen, biomass growth, nitrogen uptake and amount of N_2 fixed) in order to minimize error compensations in the simulation of the processes leading to grain yield and fixed N_2. Such procedure led to accurate simulation of grain yield and N_2 fixed under current climate (see section 3.1) and gives us confidence that water and nitrogen dynamics of the soil-crop system

505 were well simulated. However, rRMSE for simulated soil mineral nitrogen content was high
506 due to: (i) the high absolute RMSE (12 and 16 kg N ha^{-1} for calibration and evaluation dataset,
507 respectively); and (ii) the low average level of observed soil mineral nitrogen in our experiments
508 (38 and 32 kg N ha^{-1} for calibration and evaluation dataset, respectively). High RMSE of 20-35
509 kg N ha^{-1} are typical of current soil-crop models like STICS or The Agricultural Production
510 Systems sIMulator (APSIM) model (Coucheney et al., 2015; Probert et al., 1995), owing to the
511 complexity of the processes to be simulated (soil organic matter and crop residue
512 mineralization, losses through leaching and gaseous emissions and their interaction with plant
513 uptake). As a result, our calibrated model was not able to reproduce the small variations in the
514 amount of soil mineral nitrogen in the evaluation dataset. However, simulations were on
515 average in the range of the low observed values and deemed relevant for our climate impact
516 assessment.

517 Uncertainty can also be attributable to model structure (*i.e.* the mathematical equations
518 implemented in the model to account for various soil and crop processes). Impact of model
519 structure on simulation uncertainty is often evaluated with inter-comparison of models (Tao et
520 al., 2018). Ensemble modelling to quantify simulation uncertainty related to model structure
521 have developed over the past decade (Asseng et al., 2013; Falconnier et al., 2020; Fleisher et
522 al., 2017). However, these inter-comparisons focused mainly on cereals or tubers and did not
523 include legumes so far. The recent inter-comparison initiative for soybean
524 (https://agmip.org/soybean-pilot/) will allow a first evaluation of simulated response of legumes
525 to changes in [CO_2], temperature and rainfall and will hopefully help initiating further studies
526 on others grain legumes. Comparison of the STICS-simulated grain legume response to heat
527 with the response simulated by models dealing explicitly with heat stress on flower abortion
528 like CROPGRO (Boote et al., 2002) would be of particular interest.

529 We explored the impact of climate change using the projections of three climate models from
530 the wider CMIP5 ensemble (Taylor et al., 2011). Some climate models not considered here may
531 predict greater changes in temperature and/or rainfall at our study location. Some climate
532 models of the ensemble indeed predicted an increase in temperature reaching more than 4°C
533 for South Europe/Mediterranean region, and decrease of annual rainfall around 40% for the
534 long-term period (IPCC, 2013).

535 *4.4 Adaptations to climate change and avenues to extend the work*

536 Uncertainty in the magnitude and the direction of the changes in legume grain yield does not
537 preclude the design of robust adaptation options*, i.e.* that provide a yield advantage regardless
538 of the climate change scenario (Vermeulen et al., 2013). In our simulations at our study site,
539 winter legume tended to benefit more from climate change or to be less affected than the spring
540 pea cultivar. In the most constraining climate change scenarios, the risk of yield failure for the
541 latter would rise considerably (see section 3.4). Yield variability, a prominent constraint to
542 widespread adoption of grain legumes by farmers, would therefore be magnified for this crop.
543 Favoring winter over spring grain legumes therefore appears as a promising strategy to adapt
544 to future climate in southwestern France.

545 The diversity in current temperature and seasonal rainfall climate conditions is often very useful
546 in explaining crop response to climate change. Global studies show that yield losses due to rise
547 in temperature are greater at warmer locations, while impact of water stress is predicted to be
548 stronger at drier locations (Waha et al., 2013; Zhao et al., 2017). Plant-available water content
549 is also a critical soil parameter that drives the risk of water stress on crops (Whitbread et al.,
550 2017). Our study site located at the northern fringe of the Mediterranean region is characterized
551 by a cooler and wetter area compared with others regions in lower latitudes such as Spain and
552 Greece. Soils are also deep (135cm) in Auzeville. Further modelling work should focus on
553 model calibration against field data and exploration of the impact of climate change in

554 additional sentinel sites in southern locations and/or with contrasting soil types. This would
555 allow for a more comprehensive assessment of the impact of climate change on grain legumes
556 in Southern Europe. Possibly, the advantage of winter-legumes over spring legumes will be
557 magnified in sites that are warmer and drier and/or with shallower soils. Our study would
558 provide a useful basis for comparison.

559 Rise in temperature causes a decrease in crop cycle duration and therefore yield potential (see
560 section 3.5.1). Adoption of late-maturing cultivars could help to regain this reduction in the
561 length of vegetative and/or reproductive period (see Bregaglio et al., 2017 for a useful example
562 on rice). However, the trade-offs between extended crop cycle duration and possible additional
563 heat and drought stress have to be quantified. Our model calibration for pea and winter faba
564 bean could offer the opportunity to explore these trade-offs and to define best suited ideotypes
565 with optimal vegetative and reproductive growth duration that minimize abiotic stresses (see
566 Senapati et al., 2019 for a useful example on wheat and Ravasi et al., 2020 on pea). In our study,
567 sowing dates were identical in historical and future climate to isolate the effect of climate
568 change. However, explorations of ideotypes should also consider the interactions between
569 cultivar characteristics and sowing date (see Dobor et al., 2016 for an example on maize and
570 winter wheat), and notably the opportunity to sow earlier spring legume cultivars as
571 temperatures rise and winters become milder. The identification of these ideotypes can help set
572 priorities for breeders aiming at developing new cultivars adapted to climate change. Analysis
573 of current cultivar diversity (*e.g.* Bodner et al., 2018 for faba bean) will also help identify
574 specific traits that confer adaptation to heat stress. For example, Delahunty et al., (2018) showed
575 that some lentil genotypes were able to maintain grain set under high temperature. Soil
576 compaction associated with the increase in machinery weight (Keller et al., 2019) can decrease
577 root growth, soil water storage capacity and legumes N_2 fixation. Mitigation of compaction
578 effects with *e.g.* lighter machinery may help to improve soil water storage capacity and adapt

579 to plausible increases in drought stress. STICS has a specific option to account for the impact
580 of soil compaction on roots growth (Brisson et al., 2009), so that future modelling studies on
581 adaptation could incorporate options to mitigate soil compaction, provided that the STICS
582 module has been sufficiently evaluated. Irrigation could also help reduce water stress, but the
583 design of ideotypes with shifts in growth cycle to take better advantage of spring precipitations
584 could also help lower crop water requirements (Ravasi et al., 2020). Our study did not consider
585 the potential impacts of biotic factors (weeds, pests and diseases). STICS does not simulate
586 interactions between crops and parasitic /pathogenic organisms and no simulation tool for biotic
587 interactions coupled to STICS is operational yet. Yet, pea and faba bean can host above- and
588 belowground pests and pathogenic species (e.g. aphids, sitones, seed beetles, *Aschochyta*, rust,
589 *Aphanomyces*) that can significantly reduce crop yield (Rubiales et al., 2015). In the future,
590 climate change may alter these biotic threats through shifts in phenology, multi-trophic
591 relationships, distribution and severity of known biotic stressors and emergence of new ones
592 (Juroszek et al., 2020). Assessing whether these changes may have positive or negative
593 outcomes on such crops is an important complementary step, especially in the prospect of
594 sustainable agriculture, where pesticide use is reduced and pest and disease control might be
595 more uncertain (Thurman et al., 2017).

596 Eventually, if diversification with grain legume is to contribute substantially to climate change
597 adaptation, it is important that the risk associated with their integration in cropping systems is
598 transferred equitably along the value chain. The development of risk sharing instruments like
599 indemnity or index-based insurances, along with changes in diet to increase market demand are
600 examples of the needed transformative changes (Smith et al., 2019).

601 **5. Conclusion**

602 Our study shows that the STICS crop model reproduced accurately the growth, grain yield and
603 N_2 fixation of currently under-studied cool-season grain legumes like faba bean and pea under

current climate. Model simulations showed that these cool-season grain legumes would benefit from climate change, the effect of [CO_2] increase generally offsetting the negative impact of heat and drought stress on grain yield and N_2 fixation. For one constraining climate scenario with strong increase in temperature and decrease in rainfall, [CO_2] increase would however not be sufficient to offset the negative impacts of climate change and spring pea would be then more affected than winter pea and winter faba bean. Such results have to be confirmed by simulations with extended crop model ensembles to quantify the uncertainty in how models simulate the impact of [CO_2] increase, heat and drought stress on yield and N_2 fixation of these grain legumes. Our study already documents the need to adapt cultivar choice to climate change, and the opportunity to tap into the differences between spring and winter legumes for such adaptation.

Acknowledgment:

This research was supported by the European Commission (REA) through the LEGATO project (FP7-613551) and the French National Research Agency (ANR) through the LEGITIMES French project (ANR-13-AGRO-0004) and the Climate-CAFE European project (selected by the European FACCE-JPI ERA-NET Plus program).

We thank the Centre Régional de Recherche et d'Expérimentation en Agriculture Biologique de Midi-Pyrénées (CREAB-MP) in Auch, France, for making available their faba bean dataset. We are grateful to Loïc Prieur, Didier Rafaillac, Michel Labarrère and several trainees who assisted in data collection and Didier Chesneau and Eric Lecloux who performed the extraction and the analysis of soil mineral N.

References:

Affholder, F., 1997. Empirically modelling the interaction between intensification and climatic risk in semiarid regions. Field Crops Res. 52, 79–93. https://doi.org/10.1016/S0378-4290(96)03453-3

Ainsworth, E.A., Rogers, A., 2007. The response of photosynthesis and stomatal conductance to rising [CO2]: mechanisms and environmental interactions. Plant Cell Environ. 30, 258–270. https://doi.org/10.1111/j.1365-3040.2007.01641.x

Amir, J., Sinclair, T.R., 1991. A model of the temperature and solar-radiation effects on spring wheat growth and yield. Field Crops Res. 28, 47–58. https://doi.org/10.1016/0378-4290(91)90073-5

Asseng, S., Ewert, F., Rosenzweig, C., Jones, J.W., Hatfield, J.L., Ruane, A.C., Boote, K.J., Thorburn, P.J., Rötter, R.P., Cammarano, D., Brisson, N., Basso, B., Martre, P., Aggarwal, P.K., Angulo, C., Bertuzzi, P., Biernath, C., Challinor, A.J., Doltra, J., Gayler, S., Goldberg, R., Grant, R., Heng, L., Hooker, J., Hunt, L.A., Ingwersen, J., Izaurralde, R.C., Kersebaum, K.C., Müller, C., Naresh Kumar, S., Nendel, C., O'Leary, G., Olesen, J.E., Osborne, T.M., Palosuo, T., Priesack, E., Ripoche, D., Semenov, M.A., Shcherbak, I., Steduto, P., Stöckle, C., Stratonovitch, P., Streck, T., Supit, I., Tao, F., Travasso, M., Waha, K., Wallach, D., White, J.W., Williams, J.R., Wolf, J., 2013. Uncertainty in simulating wheat yields under climate change. Nat. Clim. Change 3, 827–832. https://doi.org/10.1038/nclimate1916

Asseng, S., Zhu, Y., Wang, E., Zhang, W., 2015. Chapter 20 - Crop modeling for climate change impact and adaptation, in: Sadras, V.O., Calderini, D.F. (Eds.), Crop Physiology (Second Edition). Academic Press, San Diego, pp. 505–546. https://doi.org/10.1016/B978-0-12-417104-6.00020-0

Bedoussac, L., Justes, E., 2010. Dynamic analysis of competition and complementarity for light and N use to understand the yield and the protein content of a durum wheat–winter pea intercrop. Plant Soil 330, 37–54. https://doi.org/10.1007/s11104-010-0303-8

Bergez, J.E., Raynal, H., Launay, M., Beaudoin, N., Casellas, E., Caubel, J., Chabrier, P., Coucheney, E., Dury, J., Garcia de Cortazar-Atauri, I., Justes, E., Mary, B., Ripoche, D., Ruget, F., 2014. Evolution of the STICS crop model to tackle new environmental issues: New formalisms and integration in the modelling and simulation platform RECORD. Environ. Model. Softw. 62, 370–384. https://doi.org/10.1016/j.envsoft.2014.07.010

Bishop, J., Potts, S.G., Jones, H.E., 2016. Susceptibility of Faba Bean (Vicia faba L.) to Heat Stress During Floral Development and Anthesis. J. Agron. Crop Sci. 202, 508–517. https://doi.org/10.1111/jac.12172

Boote, K.J., Mínguez, M.I., Sau, F., 2002. Adapting the CROPGRO legume model to simulate growth of faba bean. Agron. J. 94, 743–756.

Bourgault, M., Brand, J., Tausz, M., Fitzgerald, G.J., 2016. Yield, growth and grain nitrogen response to elevated CO2 of five field pea (Pisum sativum L.) cultivars in a low rainfall environment. Field Crops Res. 196, 1–9. https://doi.org/10.1016/j.fcr.2016.04.011

Bourgault, M., Löw, M., Tausz-Posch, S., Nuttall, J.G., Delahunty, A.J., Brand, J., Panozzo, J.F., McDonald, L., O'Leary, G.J., Armstrong, R.D., Fitzgerald, G.J., Tausz, M., 2018. Effect of a Heat Wave on Lentil Grown under Free-Air CO 2 Enrichment (FACE) in a Semi-Arid Environment. Crop Sci. 58, 803–812. https://doi.org/10.2135/cropsci2017.09.0565

Bregaglio, S., Hossard, L., Cappelli, G., Resmond, R., Bocchi, S., Barbier, J.-M., Ruget, F., Delmotte, S., 2017. Identifying trends and associated uncertainties in potential rice production under climate change in Mediterranean areas. Agric. For. Meteorol. 237–238, 219–232. https://doi.org/10.1016/j.agrformet.2017.02.015

Brisson, N., Launay, M., Mary, B., Beaudoin, N., 2009. Conceptual Basis, Formalisations and Parameterization of the Stics Crop Model. Editions Quae.

Brisson, N., Mary, B., Ripoche, D., Jeuffroy, M.H., Ruget, F., Nicoullaud, B., Gate, P., Devienne-Barret, F., Antonioletti, R., Durr, C., others, 1998. STICS: a generic model for the simulation of crops

675 and their water and nitrogen balances. I. Theory and parameterization applied to wheat and
676 corn. Agronomie 18, 311–346.
677 Brisson, N., Ruget, F., Gate, P., Lorgeou, J., Nicoullaud, B., Tayot, X., Plenet, D., Jeuffroy, M.-H.,
678 Bouthier, A., Ripoche, D., Mary, B., Justes, E., 2002. STICS: a generic model for simulating
679 crops and their water and nitrogen balances. II. Model validation for wheat and maize.
680 Agronomie 22, 69–92. https://doi.org/10.1051/agro:2001005
681 Carranca, C., de Varennes, A., Rolston, D., 1999. Biological nitrogen fixation by fababean, pea and
682 chickpea, under field conditions, estimated by the 15N isotope dilution technique. Eur. J.
683 Agron. 10, 49–56. https://doi.org/10.1016/S1161-0301(98)00049-5
684 Cernay, C., Ben-Ari, T., Pelzer, E., Meynard, J.-M., Makowski, D., 2015. Estimating variability in grain
685 legume yields across Europe and the Americas. Sci. Rep. 5, 11171.
686 https://doi.org/10.1038/srep11171
687 Challinor, A., Martre, P., Asseng, S., Thornton, P., Ewert, F., 2014. Making the most of climate impacts
688 ensembles. Nat. Clim. Change 4, 77–80. https://doi.org/10.1038/nclimate2117
689 Coucheney, E., Buis, S., Launay, M., Constantin, J., Mary, B., García de Cortázar-Atauri, I., Ripoche, D.,
690 Beaudoin, N., Ruget, F., Andrianarisoa, K.S., Le Bas, C., Justes, E., Léonard, J., 2015. Accuracy,
691 robustness and behavior of the STICS soil–crop model for plant, water and nitrogen outputs:
692 Evaluation over a wide range of agro-environmental conditions in France. Environ. Model.
693 Softw. 64, 177–190. https://doi.org/10.1016/j.envsoft.2014.11.024
694 Craufurd, P.Q., Wheeler, T.R., 2009. Climate change and the flowering time of annual crops. J. Exp.
695 Bot. 60, 2529–2539. https://doi.org/10.1093/jxb/erp196
696 Delahunty, A., Nuttall, J., Nicolas, M., Brand, J., 2018. Response of lentil to high temperature under
697 variable water supply and carbon dioxide enrichment. Crop Pasture Sci. 69, 1103–1112.
698 https://doi.org/10.1071/CP18004
699 Dobor, L., Barcza, Z., Hlásny, T., Árendás, T., Spitkó, T., Fodor, N., 2016. Crop planting date matters:
700 Estimation methods and effect on future yields. Agric. For. Meteorol. 223, 103–115.
701 https://doi.org/10.1016/j.agrformet.2016.03.023
702 Falconnier, G.N., Corbeels, M., Boote, K.J., Affholder, F., Adam, M., MacCarthy, D.S., Ruane, A.C.,
703 Nendel, C., Whitbread, A.M., Justes, E., Ahuja, L.R., Akinseye, F.M., Alou, I.N., Amouzou, K.A.,
704 Anapalli, S.S., Baron, C., Basso, B., Baudron, F., Bertuzzi, P., Challinor, A.J., Chen, Y., Deryng,
705 D., Elsayed, M.L., Faye, B., Gaiser, T., Galdos, M., Gayler, S., Gerardeaux, E., Giner, M., Grant,
706 B., Hoogenboom, G., Ibrahim, E.S., Kamali, B., Kersebaum, K.C., Kim, S.H., Laan, M. van der,
707 Leroux, L., Lizaso, J.I., Maestrini, B., Meier, E.A., Mequanint, F., Ndoli, A., Porter, C.H.,
708 Priesack, E., Ripoche, D., Sida, T., Singh, U., Smith, W., Srivastava, A., Sinha, S., Tao, F.,
709 Thorburn, P.J., Timlin, D., Traore, B., Twine, T., Webber, H., 2020. Modelling climate change
710 impacts on maize yields under low nitrogen input conditions in sub-Saharan Africa. Glob.
711 Change Biol. n/a. https://doi.org/10.1111/gcb.15261
712 Falconnier, G.N., Journet, E.-P., Bedoussac, L., Vermue, A., Chlébowski, F., Beaudoin, N., Justes, E.,
713 2019. Calibration and evaluation of the STICS soil-crop model for faba bean to explain
714 variability in yield and N2 fixation. Eur. J. Agron. 104, 63–77.
715 https://doi.org/10.1016/j.eja.2019.01.001
716 Faye, B., Webber, H., Diop, M., Mbaye, M.L., Owusu-Sekyere, J.D., Naab, J.B., Gaiser, T., 2018.
717 Potential impact of climate change on peanut yield in Senegal, West Africa. Field Crops Res.
718 219, 148–159. https://doi.org/10.1016/j.fcr.2018.01.034
719 Fleisher, D.H., Condori, B., Quiroz, R., Alva, A., Asseng, S., Barreda, C., Bindi, M., Boote, K.J., Ferrise,
720 R., Franke, A.C., Govindakrishnan, P.M., Harahagazwe, D., Hoogenboom, G., Kumar, S.N.,
721 Merante, P., Nendel, C., Olesen, J.E., Parker, P.S., Raes, D., Raymundo, R., Ruane, A.C.,
722 Stockle, C., Supit, I., Vanuytrecht, E., Wolf, J., Woli, P., 2017. A potato model intercomparison
723 across varying climates and productivity levels. Glob. Change Biol. 23, 1258–1281.
724 https://doi.org/10.1111/gcb.13411
725 Foyer, C.H., Lam, H.-M., Nguyen, H.T., Siddique, K.H.M., Varshney, R.K., Colmer, T.D., Cowling, W.,
726 Bramley, H., Mori, T.A., Hodgson, J.M., Cooper, J.W., Miller, A.J., Kunert, K., Vorster, J., Cullis,

C., Ozga, J.A., Wahlqvist, M.L., Liang, Y., Shou, H., Shi, K., Yu, J., Fodor, N., Kaiser, B.N., Wong, F.-L., Valliyodan, B., Considine, M.J., 2016. Neglecting legumes has compromised human health and sustainable food production. Nat. Plants 2, 16112. https://doi.org/10.1038/nplants.2016.112

Gammans, M., Mérel, P., Ortiz-Bobea, A., 2017. Negative impacts of climate change on cereal yields: statistical evidence from France. Environ. Res. Lett. 12, 054007. https://doi.org/10.1088/1748-9326/aa6b0c

Gijsman, A.J., Jagtap, S.S., Jones, J.W., 2002. Wading through a swamp of complete confusion: how to choose a method for estimating soil water retention parameters for crop models. Eur. J. Agron., Process Simulation and Application of Cropping System Models 18, 77–106. https://doi.org/10.1016/S1161-0301(02)00098-9

Giorgi, F., 2006. Climate change hot-spots. Geophys. Res. Lett. 33, L08707. https://doi.org/10.1029/2006GL025734

Guan, K., Sultan, B., Biasutti, M., Baron, C., Lobell, D.B., 2017. Assessing climate adaptation options and uncertainties for cereal systems in West Africa. Agric. For. Meteorol. 232, 291–305. https://doi.org/10.1016/j.agrformet.2016.07.021

Guillaume, S., Bergez, J.-E., Wallach, D., Justes, E., 2011. Methodological comparison of calibration procedures for durum wheat parameters in the STICS model. Eur. J. Agron. 35, 115–126. https://doi.org/10.1016/j.eja.2011.05.003

IPCC, 2013. Annex I: Atlas of Global and Regional Climate Projections, in: van Oldenborgh, G.J., Collins, J., Arblaster, J., Christensen, J., Marotzke, J., Power, S.B., Rummukainen, M., Zhou, T. (Eds.), Climate Change 2013: The Physical Science Basis. Contribution of Working Group I to the Fifth Assessment Report of the Intergovernmental Panel on Climate Change. Cambridge University Press, Cambridge, United Kingdom and New York, NY, US.

Jacob, D., Petersen, J., Eggert, B., Alias, A., Christensen, O.B., Bouwer, L.M., Braun, A., Colette, A., Déqué, M., Georgievski, G., Georgopoulou, E., Gobiet, A., Menut, L., Nikulin, G., Haensler, A., Hempelmann, N., Jones, C., Keuler, K., Kovats, S., Kröner, N., Kotlarski, S., Kriegsmann, A., Martin, E., Meijgaard, E. van, Moseley, C., Pfeifer, S., Preuschmann, S., Radermacher, C., Radtke, K., Rechid, D., Rounsevell, M., Samuelsson, P., Somot, S., Soussana, J.-F., Teichmann, C., Valentini, R., Vautard, R., Weber, B., Yiou, P., 2014. EURO-CORDEX: new high-resolution climate change projections for European impact research. Reg. Environ. Change 14, 563–578. https://doi.org/10.1007/s10113-013-0499-2

Jégo, G., Pattey, E., Bourgeois, G., Morrison, M.J., Drury, C.F., Tremblay, N., Tremblay, G., 2010. Calibration and performance evaluation of soybean and spring wheat cultivars using the STICS crop model in Eastern Canada. Field Crops Res. 117, 183–196. https://doi.org/10.1016/j.fcr.2010.03.008

Juroszek, P., Racca, P., Link, S., Farhumand, J., Kleinhenz, B., 2020. Overview on the review articles published during the past 30 years relating to the potential climate change effects on plant pathogens and crop disease risks. Plant Pathol. 69, 179–193. https://doi.org/10.1111/ppa.13119

Kammoun, B., 2014. Analyse des interactions génotype x environnement x conduite culturale de peuplement bi-spécifique de cultures associées de blé dur et de légumineuses à graines, à des fins de choix variétal et d'optimisation de leurs itinéraires techniques. École Doctorale Sciences Écologiques, Vétérinaires, Agronomiques et Bioingénieries (Toulouse); 154236330.

Karrou, M., Oweis, T., 2012. Water and land productivities of wheat and food legumes with deficit supplemental irrigation in a Mediterranean environment. Agric. Water Manag. 107, 94–103. https://doi.org/10.1016/j.agwat.2012.01.014

Lemaire, G., Gastal, F., 1997. N Uptake and Distribution in Plant Canopies, in: Diagnosis of the Nitrogen Status in Crops. Springer, Berlin, Heidelberg, pp. 3–43. https://doi.org/10.1007/978-3-642-60684-7_1

Martre, P., Wallach, D., Asseng, S., Ewert, F., Jones, J.W., Rötter, R.P., Boote, K.J., Ruane, A.C., Thorburn, P.J., Cammarano, D., Hatfield, J.L., Rosenzweig, C., Aggarwal, P.K., Angulo, C.,

779 Basso, B., Bertuzzi, P., Biernath, C., Brisson, N., Challinor, A.J., Doltra, J., Gayler, S., Goldberg,
780 R., Grant, R.F., Heng, L., Hooker, J., Hunt, L.A., Ingwersen, J., Izaurralde, R.C., Kersebaum,
781 K.C., Müller, C., Kumar, S.N., Nendel, C., O'leary, G., Olesen, J.E., Osborne, T.M., Palosuo, T.,
782 Priesack, E., Ripoche, D., Semenov, M.A., Shcherbak, I., Steduto, P., Stöckle, C.O.,
783 Stratonovitch, P., Streck, T., Supit, I., Tao, F., Travasso, M., Waha, K., White, J.W., Wolf, J.,
784 2015. Multimodel ensembles of wheat growth: many models are better than one. Glob.
785 Change Biol. 21, 911–925. https://doi.org/10.1111/gcb.12768
786 McDonald, G.K., Paulsen, G.M., 1997. High temperature effects on photosynthesis and water
787 relations of grain legumes. Plant Soil 196, 47–58. https://doi.org/10.1023/A:1004249200050
788 Mohammed, A., Tana, T., Singh, P., Molla, A., Seid, A., 2017. Identifying best crop management
789 practices for chickpea (Cicer arietinum L.) in Northeastern Ethiopia under climate change
790 condition. Agric. Water Manag. 194, 68–77. https://doi.org/10.1016/j.agwat.2017.08.022
791 Neugschwandtner, R.W., Bernhuber, A., Kammlander, S., Wagentristl, H., Klimek-Kopyra, A., Kaul, H.-
792 P., 2019. Agronomic potential of winter grain legumes for Central Europe: Development, soil
793 coverage and yields. Field Crops Res. 241, 107576. https://doi.org/10.1016/j.fcr.2019.107576
794 Parvin, S., Uddin, S., Tausz-Posch, S., Fitzgerald, G., Armstrong, R., Tausz, M., 2019. Elevated CO2
795 improves yield and N2 fixation but not grain N concentration of faba bean (Vicia faba L.)
796 subjected to terminal drought. Environ. Exp. Bot. 165, 161–173.
797 https://doi.org/10.1016/j.envexpbot.2019.06.003
798 Peel, M.C., Finlayson, B.L., McMahon, T.A., 2007. Updated world map of the Köppen-Geiger climate
799 classification. Hydrol Earth Syst Sci 11, 1633–1644. https://doi.org/10.5194/hess-11-1633-
800 2007
801 Plaza-Bonilla, D., Nolot, J.-M., Raffaillac, D., Justes, E., 2017. Innovative cropping systems to reduce N
802 inputs and maintain wheat yields by inserting grain legumes and cover crops in southwestern
803 France. Eur. J. Agron. 82, Part B, 331–341. https://doi.org/10.1016/j.eja.2016.05.010
804 Prasad, P.V.V., Boote, K.J., Allen, L.H., Thomas, J.M.G., 2002. Effects of elevated temperature and
805 carbon dioxide on seed-set and yield of kidney bean (Phaseolus vulgaris L.). Glob. Change
806 Biol. 8, 710–721. https://doi.org/10.1046/j.1365-2486.2002.00508.x
807 Probert, M.E., Keating, B.A., Thompson, J.P., Parton, W.J., 1995. Modelling water, nitrogen, and crop
808 yield for a long-term fallow management experiment. Aust. J. Exp. Agric. 35, 941–950.
809 https://doi.org/10.1071/ea9950941
810 Ravasi, R.A., Paleari, L., Vesely, F.M., Movedi, E., Thoelke, W., Confalonieri, R., 2020. Ideotype
811 definition to adapt legumes to climate change: A case study for field pea in Northern Italy.
812 Agric. For. Meteorol. 291, 108081. https://doi.org/10.1016/j.agrformet.2020.108081
813 Rogers, A., Ainsworth, E.A., Leakey, A.D.B., 2009. Will Elevated Carbon Dioxide Concentration Amplify
814 the Benefits of Nitrogen Fixation in Legumes? Plant Physiol. 151, 1009–1016.
815 https://doi.org/10.1104/pp.109.144113
816 Rubiales, D., Fondevilla, S., Chen, W., Gentzbittel, L., Higgins, T.J.V., Castillejo, M.A., Singh, K.B.,
817 Rispail, N., 2015. Achievements and Challenges in Legume Breeding for Pest and Disease
818 Resistance. Crit. Rev. Plant Sci. 34, 195–236. https://doi.org/10.1080/07352689.2014.898445
819 Saxton, K.E., Rawls, W.J., 2006. Soil water characteristic estimates by texture and organic matter for
820 hydrologic solutions. Soil Sci. Soc. Am. J. 70, 1569–1578.
821 https://doi.org/10.2136/sssaj2005.0117
822 Senapati, N., Brown, H.E., Semenov, M.A., 2019. Raising genetic yield potential in high productive
823 countries: Designing wheat ideotypes under climate change. Agric. For. Meteorol. 271, 33–
824 45. https://doi.org/10.1016/j.agrformet.2019.02.025
825 Smith, P., Calvin, K., Nkem, J., Campbell, D., Cherubini, F., Grassi, G., Korotkov, V., Hoang, A.L., Lwasa,
826 S., McElwee, P., Nkonya, E., Saigusa, N., Soussana, J.-F., Angel Taboada, M., Manning, F.C.,
827 Nampanzira, D., Arias-Navarro, C., Vizzarri, M., House, J., Roe, S., Cowie, A., Rounsevell, M.,
828 Arneth, A., n.d. Which practices co-deliver food security, climate change mitigation and
829 adaptation, and combat land degradation and desertification? Glob. Change Biol.
830 https://doi.org/10.1111/gcb.14878

Tao, F., Rötter, R.P., Palosuo, T., Díaz-Ambrona, C.G.H., Mínguez, M.I., Semenov, M.A., Kersebaum, K.C., Nendel, C., Specka, X., Hoffmann, H., Ewert, F., Dambreville, A., Martre, P., Rodríguez, L., Ruiz-Ramos, M., Gaiser, T., Höhn, J.G., Salo, T., Ferrise, R., Bindi, M., Cammarano, D., Schulman, A.H., 2018. Contribution of crop model structure, parameters and climate projections to uncertainty in climate change impact assessments. Glob. Change Biol. 24, 1291–1307. https://doi.org/10.1111/gcb.14019

Taylor, K.E., Stouffer, R.J., Meehl, G.A., 2011. An Overview of CMIP5 and the Experiment Design. Bull. Am. Meteorol. Soc. 93, 485–498. https://doi.org/10.1175/BAMS-D-11-00094.1

Themeßl, M.J., Gobiet, A., Leuprecht, A., 2011. Empirical-statistical downscaling and error correction of daily precipitation from regional climate models. Int. J. Climatol. 31, 1530–1544. https://doi.org/10.1002/joc.2168

Thurman, J.H., Crowder, D.W., Northfield, T.D., 2017. Biological control agents in the Anthropocene: current risks and future options. Curr. Opin. Insect Sci., Global change biology * Molecular physiology 23, 59–64. https://doi.org/10.1016/j.cois.2017.07.006

Vermeulen, S.J., Challinor, A.J., Thornton, P.K., Campbell, B.M., Eriyagama, N., Vervoort, J.M., Kinyangi, J., Jarvis, A., Laderach, P., Ramirez-Villegas, J., Nicklin, K.J., Hawkins, E., Smith, D.R., 2013. Addressing uncertainty in adaptation planning for agriculture. Proc. Natl. Acad. Sci. 110, 8357–8362. https://doi.org/10.1073/pnas.1219441110

Vuuren, D.P. van, Edmonds, J., Kainuma, M., Riahi, K., Thomson, A., Hibbard, K., Hurtt, G.C., Kram, T., Krey, V., Lamarque, J.-F., Masui, T., Meinshausen, M., Nakicenovic, N., Smith, S.J., Rose, S.K., 2011. The representative concentration pathways: an overview. Clim. Change 109, 5. https://doi.org/10.1007/s10584-011-0148-z

Waha, K., Müller, C., Rolinski, S., 2013. Separate and combined effects of temperature and precipitation change on maize yields in sub-Saharan Africa for mid- to late-21st century. Glob. Planet. Change 106, 1–12. https://doi.org/10.1016/j.gloplacha.2013.02.009

Wallach, D., Buis, S., Lecharpentier, P., Bourges, J., Clastre, P., Launay, M., Bergez, J.-E., Guerif, M., Soudais, J., Justes, E., 2011. A package of parameter estimation methods and implementation for the STICS crop-soil model. Environ. Model. Softw. 26, 386–394. https://doi.org/10.1016/j.envsoft.2010.09.004

Wallach, D., Palosuo, T., Thorburn, P., Seidel, S.J., Gourdain, E., Asseng, S., Basso, B., Buis, S., Crout, N., Dibari, C., Dumont, B., Ferrise, R., Gaiser, T., Garcia, C., Gayler, S., Ghahramani, A., Hochman, Z., Hoek, S., Horan, H., Hoogenboom, G., Huang, M., Jabloun, M., Jing, Q., Justes, E., Kersebaum, K.C., Klosterhalfen, A., Launay, M., Luo, Q., Maestrini, B., Moriondo, M., Zadeh, H.N., Olesen, J.E., Poyda, A., Priesack, E., Pullens, J.W.M., Qian, B., Schütze, N., Shelia, V., Souissi, A., Specka, X., Srivastava, A.K., Stella, T., Streck, T., Trombi, G., Wallor, E., Wang, J., Weber, T.K.D., Weihermüller, L., Wit, A. de, Wöhling, T., Xiao, L., Zhao, C., Zhu, Y., 2019. How well do crop models predict phenology, with emphasis on the effect of calibration? bioRxiv 708578. https://doi.org/10.1101/708578

Wang, D., Heckathorn, S.A., Wang, X., Philpott, S.M., 2012. A meta-analysis of plant physiological and growth responses to temperature and elevated CO<Subscript>2</Subscript>. Oecologia 169, 1–13. https://doi.org/10.1007/s00442-011-2172-0

Watson, C.A., Reckling, M., Preissel, S., Bachinger, J., Bergkvist, G., Kuhlman, T., Lindström, K., Nemecek, T., Topp, C.F.E., Vanhatalo, A., Zander, P., Murphy-Bokern, D., Stoddard, F.L., 2017. Grain Legume Production and Use in European Agricultural Systems. Adv. Agron. 144, 235–303. https://doi.org/10.1016/bs.agron.2017.03.003

Webber, H., Ewert, F., Olesen, J.E., Müller, C., Fronzek, S., Ruane, A.C., Bourgault, M., Martre, P., Ababaei, B., Bindi, M., Ferrise, R., Finger, R., Fodor, N., Gabaldón-Leal, C., Gaiser, T., Jabloun, M., Kersebaum, K.-C., Lizaso, J.I., Lorite, I.J., Manceau, L., Moriondo, M., Nendel, C., Rodríguez, A., Ruiz-Ramos, M., Semenov, M.A., Siebert, S., Stella, T., Stratonovitch, P., Trombi, G., Wallach, D., 2018. Diverging importance of drought stress for maize and winter wheat in Europe. Nat. Commun. 9, 1–10. https://doi.org/10.1038/s41467-018-06525-2

Whitbread, A.M., Hoffmann, M.P., Davoren, C.W., Mowat, D., Baldock, J.A., 2017. Measuring and Modeling the Water Balance in Low-Rainfall Cropping Systems. Trans. ASABE 60, 2097–2110. https://doi.org/10.13031/trans.12581

Zhao, C., Liu, B., Piao, S., Wang, X., Lobell, D.B., Huang, Y., Huang, M., Yao, Y., Bassu, S., Ciais, P., Durand, J.-L., Elliott, J., Ewert, F., Janssens, I.A., Li, T., Lin, E., Liu, Q., Martre, P., Müller, C., Peng, S., Peñuelas, J., Ruane, A.C., Wallach, D., Wang, T., Wu, D., Liu, Z., Zhu, Y., Zhu, Z., Asseng, S., 2017. Temperature increase reduces global yields of major crops in four independent estimates. Proc. Natl. Acad. Sci. 114, 9326–9331. https://doi.org/10.1073/pnas.1701762114

Figures

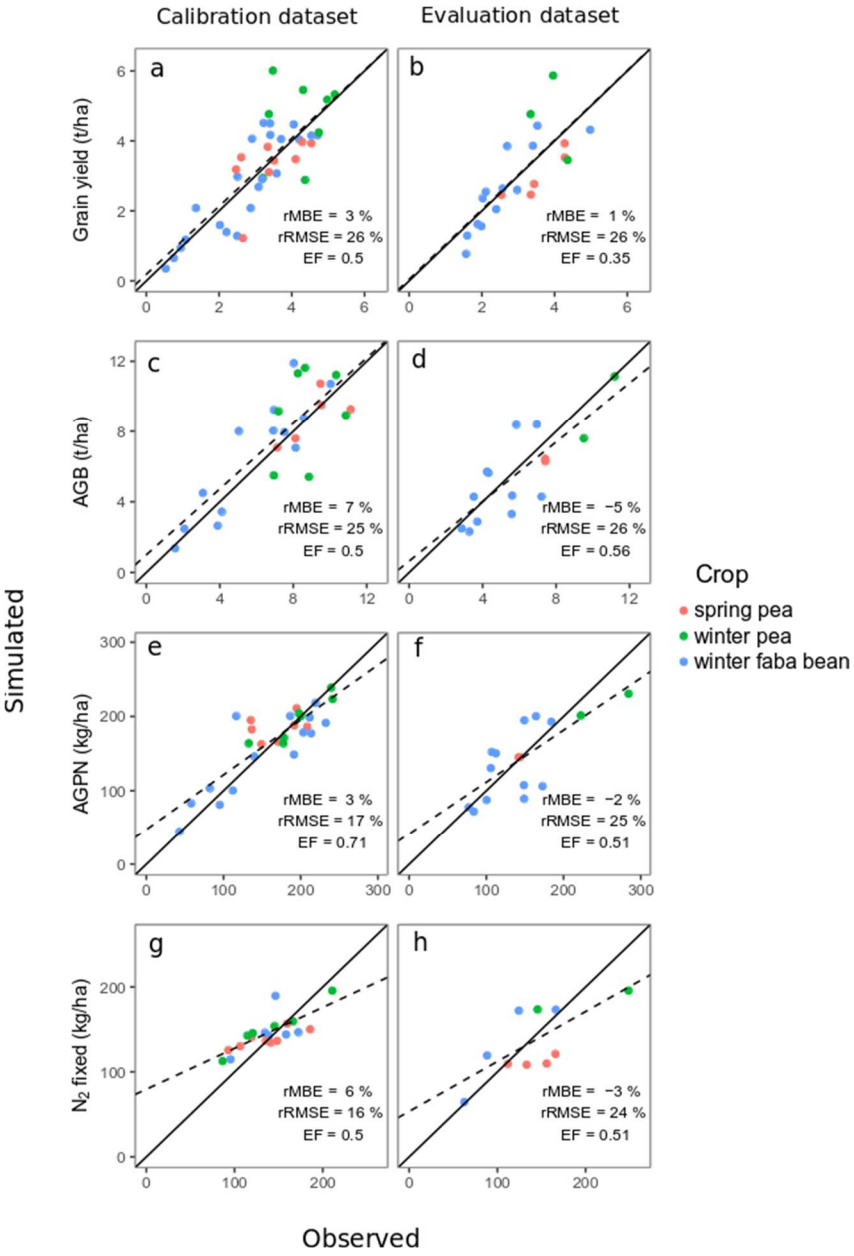

Figure 1: Comparison of observed and simulated crop variables for grain yield (a,b), above ground biomass (AGB) (c,d), above ground plant N (AGPN) (e,f) and amount of N_2 fixed at harvest (g,h), for calibration (a,c,e,g) and evaluation datasets (b,d,f,h) for spring pea (red), winter pea (green) and winter faba bean (blue). rMBE = relative mean bias error, rRMSE = relative Root Mean Square Error, EF = Efficiency. The black line is the 1:1 line. The dotted line represents the regression of simulated against observed values. The reader is referred to the web version of this article for interpretation of references to colors.

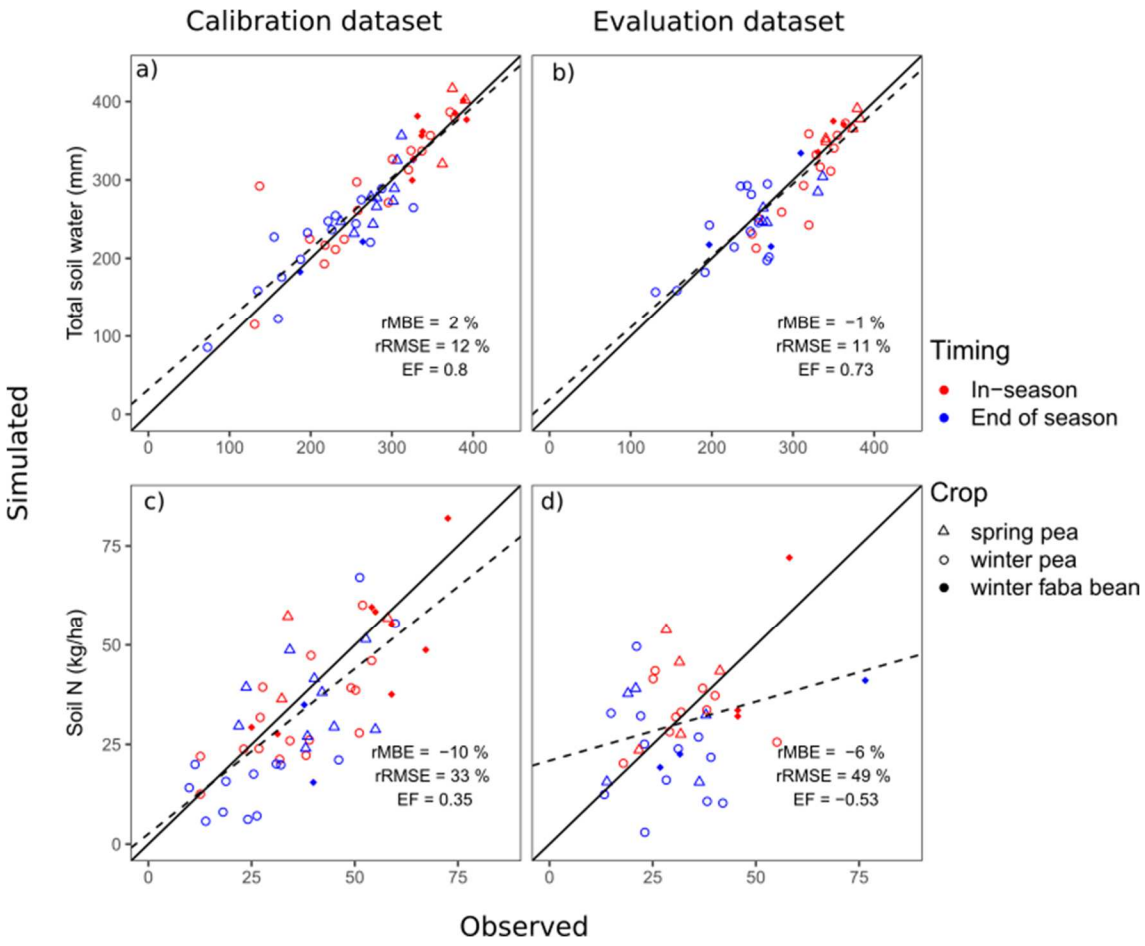

Figure 2: Comparison of observed and simulated soil variables: total soil water content (a,b) and total soil nitrogen content (c,d) for calibration (a,c) and evaluation datasets (b,d) for spring pea (triangles), winter pea (open circles) and winter faba bean (close circles), for in-season (red) and end of season measurements (blue). rMBE = relative mean bias error, rRMSE = relative Root Mean Square Error, EF=Efficiency. The black line is the 1:1 line. The dotted line represents the regression of simulated against observed values. The reader is referred to the web version of this article for interpretation of references to colors

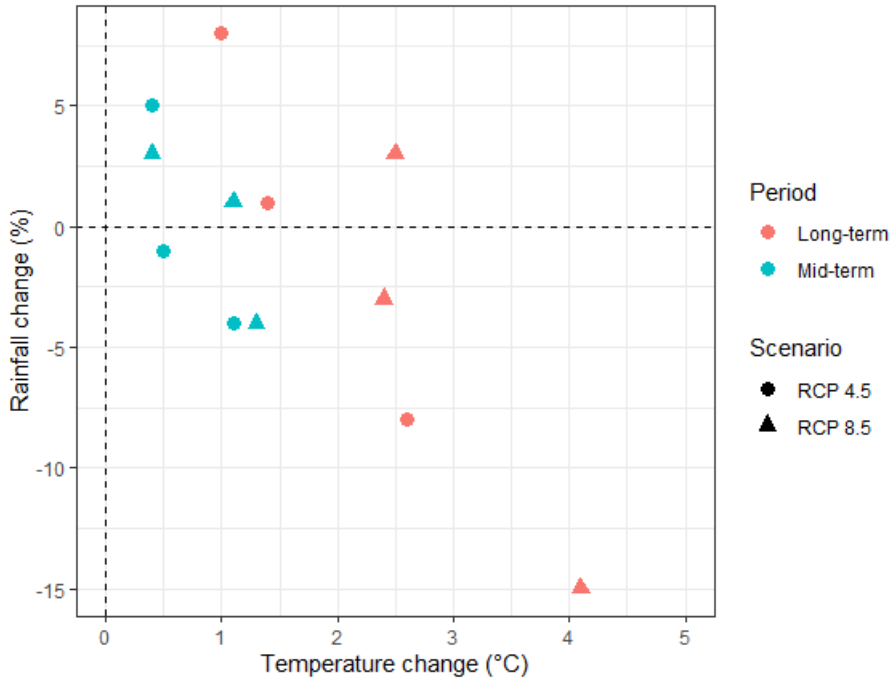

Figure 3: Change in cumulative rainfall and temperature (averaged across grain legume growing season corresponding to November-June period) as projected by three climate models under two greenhouse gas emission scenarios (Representative Concentration Pathways; RCP 4.5 with circles and RCP 8.5 with triangles) and two projections mid-term (2020-2040 in blue) and long-term (2060-2080 in red).The reader is referred to the web version of this article for interpretation of references to colors

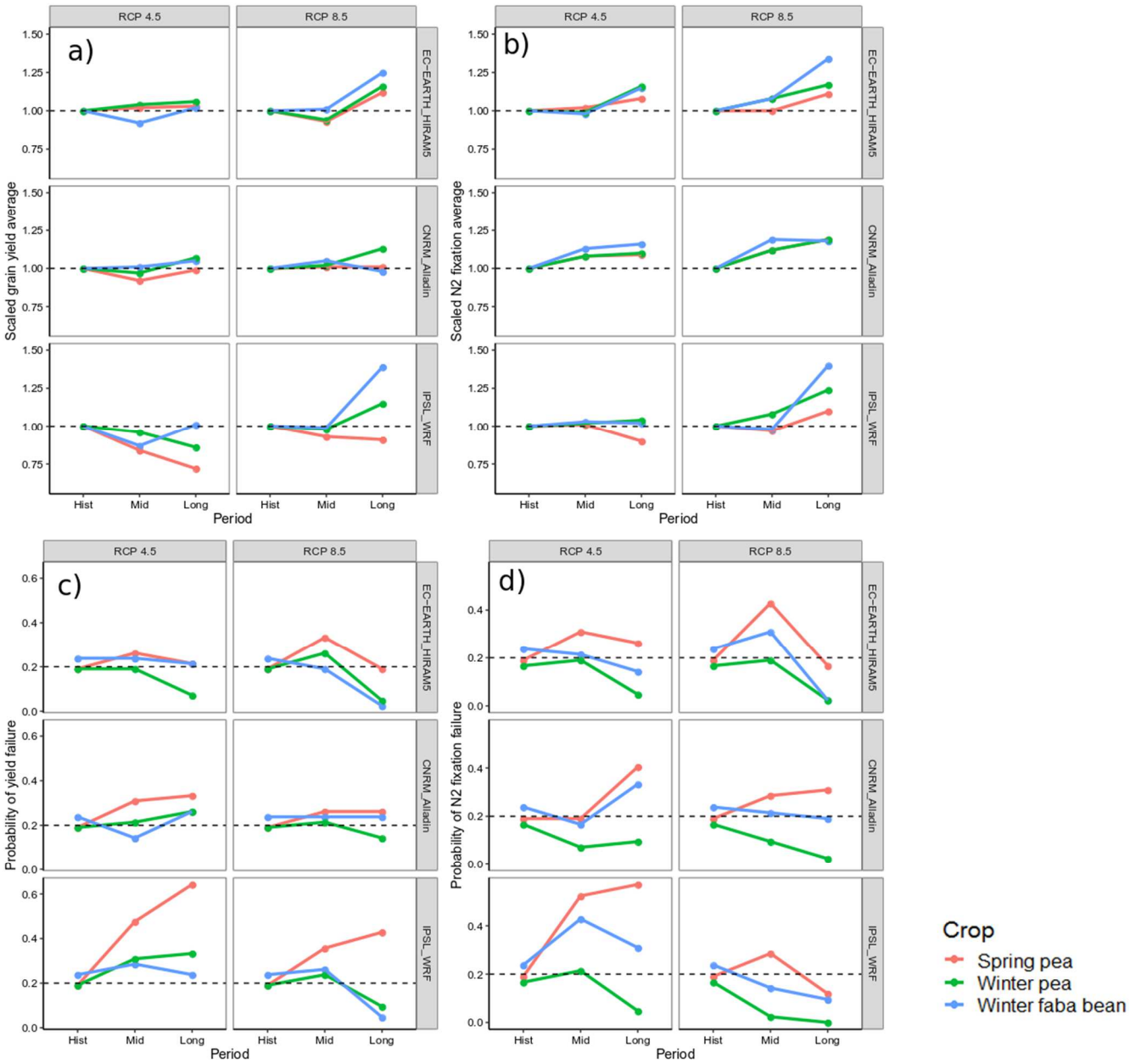

Figure 4: Scaled simulations of grain yield (a), N_2 fixation (b) and their respective risks of failure (c, d) under historical climate (Hist) (1995-2005), mid-term (Mid) (2020-2040) and long-term (Long) projections (2060-2080) for three climate models under two greenhouse gas emission scenarios (Representative Concentration Pathways; RCP 4.5 and RCP 8.5) at one location in the southwestern France for three grain legumes (spring pea in red, winter pea in green and winter faba bean in blue). The dotted horizontal line is the probability of yield failure with historical climate. The reader is referred to the web version of this article for interpretation of references to colors.

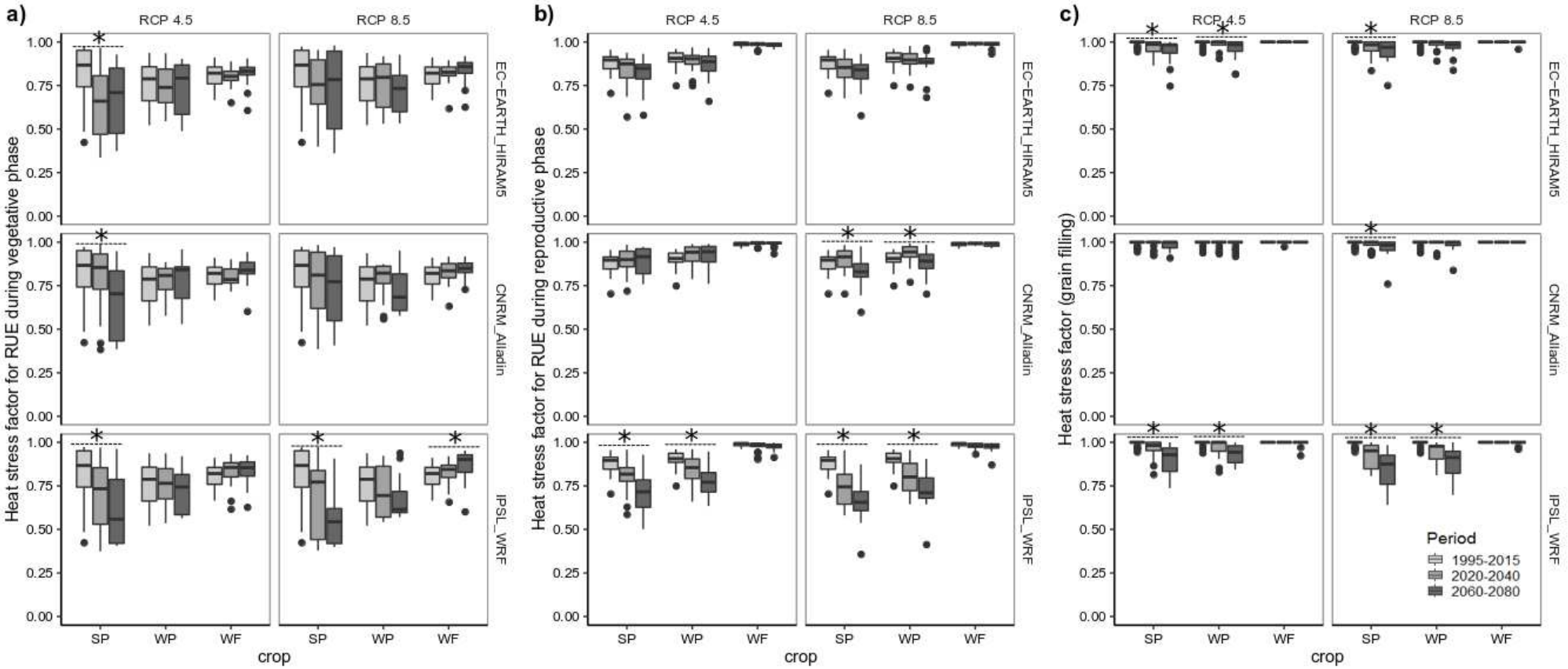

Figure 5: Simulated thermal stress factor for radiation use efficiency (RUE) during vegetative (a) and reproductive (b) phase and heat stress on grain filling (c) for historical climate, mid-term and long-term projections according to three climate models under two greenhouse gas emission scenarios (Representative Concentration Pathways; RCP 4.5 and RCP 8.5) for spring pea (SP), winter pea (WP) and winter faba bean (WF) in one location in southwestern France. Significant (P<0.05) effect of the period (historical, mid-term and long-term) on the simulated stress factor (for a given RCP and climate model) are indicated with a star on top of boxplots. For stress factors, a value of 1 indicates no stress while a value of 0 indicated maximum stress.

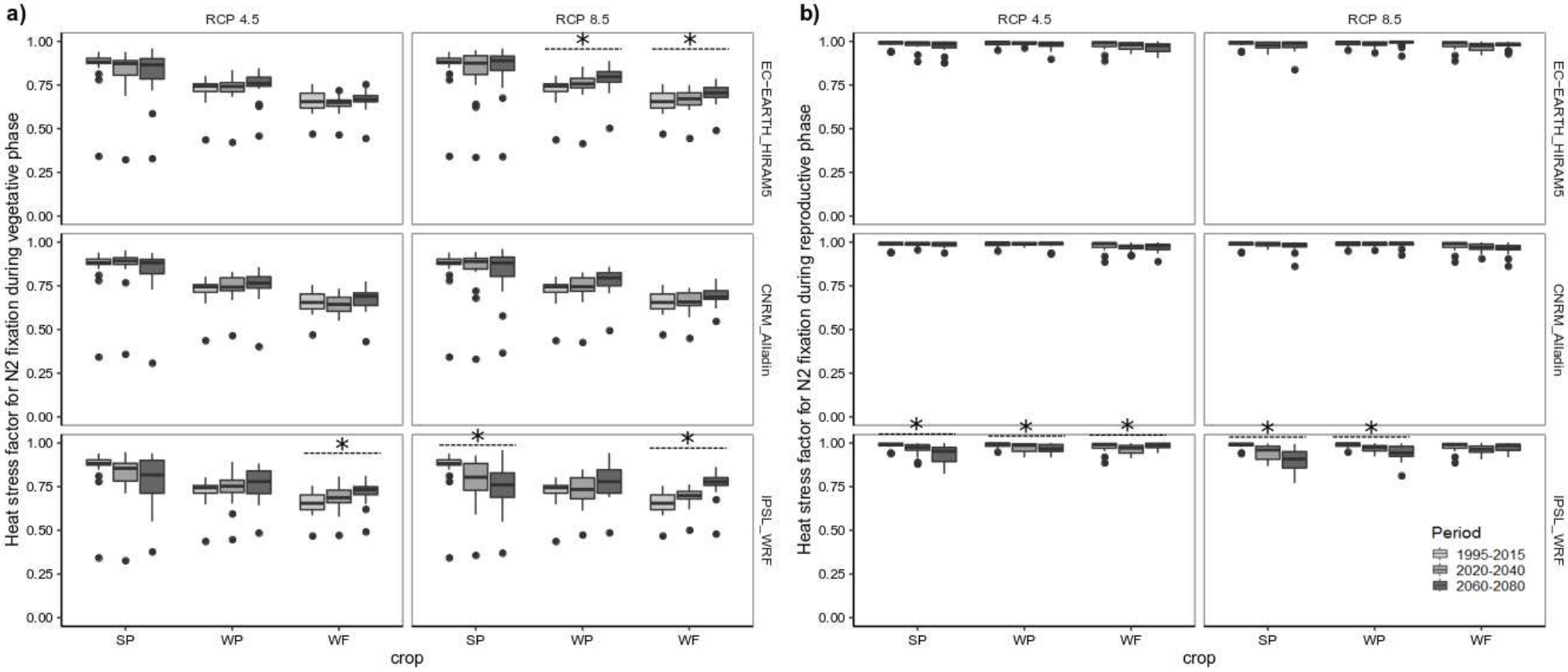

Figure 6: Simulated thermal stress factor for N_2 fixation during vegetative (a) and reproductive (b) phase for historical climate, mid-term and long-term projections according to three climate models under two greenhouse gas emission scenarios (Representative Concentration Pathways; RCP 4.5 and RCP 8.5) for spring pea (SP), winter pea (WP) and winter faba bean (WF) in one location in southwestern France. Significant (P<0.05) effect of the period (historical, mid-term and long-term) on the simulated stress factor (for a given RCP and climate model) are indicated with a star on top of boxplots. For stress factors, a value of 1 indicates no stress while a value of 0 indicated high stress.

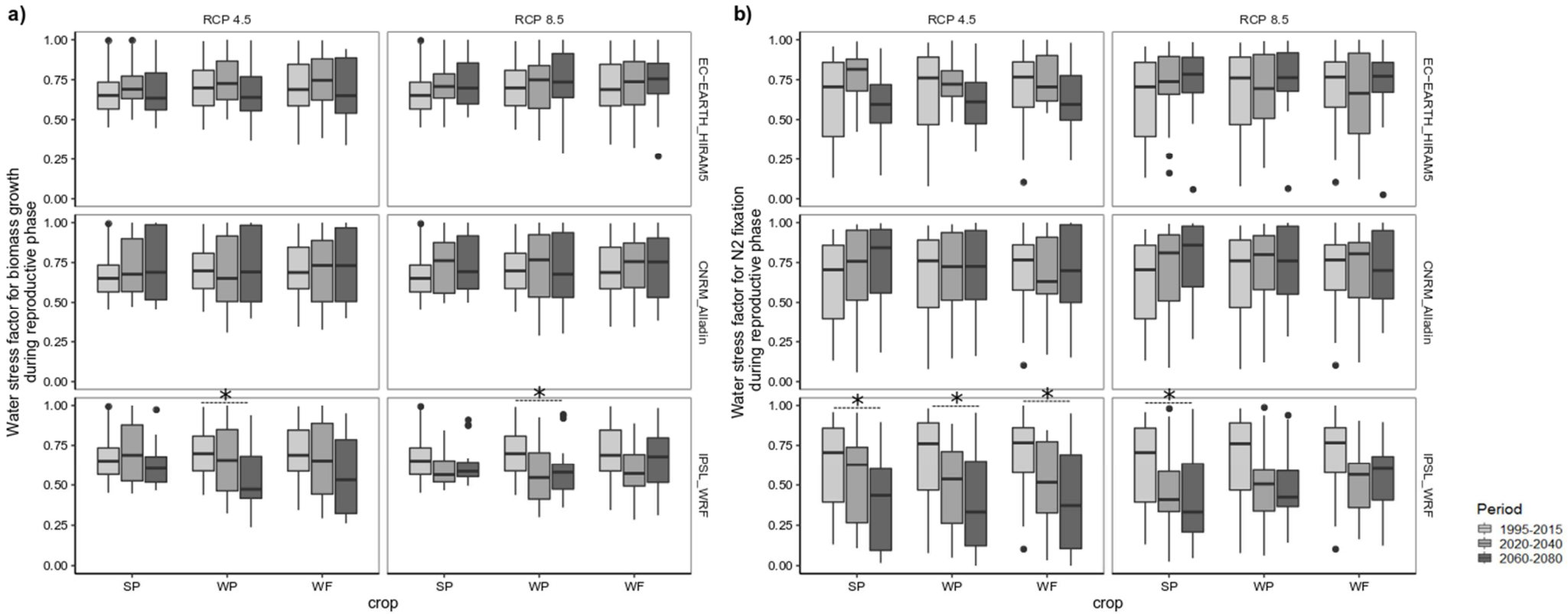

Figure 7: Simulated water stress factor for biomass growth (ratio of actual to potential transpiration) (a) and water stress on N_2 fixation (b), during reproductive phase, for historical climate, mid-term and long-term projections according to three climate models under two greenhouse gas emission scenarios (Representative Concentration Pathways; RCP 4.5 and RCP 8.5) for spring pea (SP), winter pea (WP) and winter faba bean (WF) at one location in southwestern France. Significant (P<0.05) effect of the period (historical, mid-term and long-term) on the simulated stress factor (for a given RCP and climate model) are indicated with a star on top of boxplots. For stress factors, a value of 1 indicates no stress while a value of 0 indicated high stress.

Tables

Table 1: Change in maximum and average temperatures (averaged across grain legume growing season, *i.e.* November to June) as projected by three climate models for two greenhouse gas emission scenarios (Representative Concentration Pathways; RCP 4.5 and RCP 8.5).

Variable	Scenario	Climate model	Change in temperature between 2020-2040 and historical climate (1995-2015) (°C)	Change in temperature between 2060-2080 and historical climate (1995-2015) (°C)
Maximum temperature (°C)	RCP 4.5	CNRM_Alladin	0.3	1.0
		EC-EARTH_HIRAM5	0.6	1.5
		IPSL_WRF	1.1	2.8
	RCP 8.5	CNRM_Alladin	0.5	2.7
		EC-EARTH_HIRAM5	1.5	2.9
		IPSL_WRF	1.5	4.4
Average temperature (°C)	RCP 4.5	CNRM_Alladin	0.4	1.0
		EC-EARTH_HIRAM5	0.5	1.4
		IPSL_WRF	1.1	2.6
	RCP 8.5	CNRM_Alladin	0.4	2.4
		EC-EARTH_HIRAM5	1.1	2.5
		IPSL_WRF	1.3	4.1

Table 2: Change in cumulative rainfall (averaged across grain legume growing season, *i.e.* November to June) as projected by three climate models under two greenhouse gas emission scenarios (Representative Concentration Pathways; RCP 4.5 and RCP 8.5)

Variable	Scenario	Climate model	Relative change in rainfall between 2020-2040 and historical climate (1995-2015)	Relative change in rainfall between 2060-2080 and historical climate (1995-2015)
Rainfall (mm)	RCP 4.5	CNRM_Alladin	5%	8%
		EC-EARTH_HIRAM5	-1%	1%
		IPSL_WRF	-4%	-8%
	RCP 8.5	CNRM_Alladin	3%	-3%
		EC-EARTH_HIRAM5	1%	3%
		IPSL_WRF	-4%	-15%

Table 3: Change in average simulated crop cycle duration for future climates, as projected by three climate models under two greenhouse gas emission scenarios (Representative Concentration Pathways; RCP 4.5 and RCP 8.5).

Rcp	Gcm	Crop	Change in average crop cycle duration between 2020-2040 and historical climate (1995-2015) (days)	Change in average crop cycle duration between 2060-2080 and historical climate (1995-2015) (days)
RCP 4.5	CNRM_Alladin	Spring pea	-2	-3
		Winter faba bean	-3	-5
		Winter pea	-1	-2
	EC-EARTH-HIRAM5	Spring pea	1	-6
		Winter faba bean	-3	-10
		Winter pea	-1	-7
	IPSL_WRF	Spring pea	-7	-20
		Winter faba bean	-10	-26
		Winter pea	-8	-20
RCP 8.5	CNRM_Alladin	Spring pea	0	-12
		Winter faba bean	-2	-17
		Winter pea	0	-10
	EC-EARTH-HIRAM5	Spring pea	-4	-12
		Winter faba bean	-7	-17
		Winter pea	-3	-11
	IPSL_WRF	Spring pea	-11	-29
		Winter faba bean	-14	-35
		Winter pea	-12	-28

Table 4: Relative change in simulated thermal and water stress factors between long term projections (2060 – 2080) and historical climate of three climate models under two greenhouse gas emission scenarios (Representative Concentration Pathways; RCP 4.5 and RCP 8.5) for spring pea, winter pea and winter faba bean at one location in southwestern France. Relative changes corresponding to a significant (P<0.05) effect of the period on the simulated stress factor are indicated in bold. A decrease in the simulated stress factor value indicates an increase in the stress.

			Heat stress factor					Water stress factor			
rcp	gcm	crop	RUE-vegetative phase	RUE-reproductive phase	Grain filling	N_2 fixation - Vegetative phase	N_2 fixation - Reproductive phase	Growth - vegetative phase	Growth - reproductive phase	N_2 fixation - vegetative phase	N_2 fixation - Reproductive phase
RCP 4.5	CNRM_Alladin	Spring pea	**-18%**	1%	-1%	-2%	0%	0%	9%	13%	14%
		Winter faba bean	2%	0%	0%	3%	-1%	1%	3%	3%	6%
		Winter pea	3%	2%	0%	4%	0%	1%	4%	5%	6%
	EC-EARTH_HIRAM6	Spring pea	**-20%**	-7%	**-4%**	-5%	-2%	0%	0%	4%	-6%
		Winter faba bean	1%	-1%	0%	2%	-2%	2%	-1%	0%	-7%
		Winter pea	-3%	-3%	**-3%**	4%	-1%	1%	-3%	1%	-2%
	IPSL_WRF	Spring pea	**-24%**	**-20%**	**-10%**	-9%	**-6%**	-2%	-9%	-13%	**-39%**
		Winter faba bean	2%	-1%	0%	**11%**	**0%**	-1%	-20%	-6%	**-36%**
		Winter pea	-5%	**-14%**	**-6%**	7%	**-2%**	-1%	**-23%**	-9%	**-38%**
RCP 8.5	CNRM_Alladin	Spring pea	-13%	**-6%**	**-2%**	-2%	-1%	-1%	10%	13%	17%
		Winter faba bean	5%	0%	0%	6%	-2%	0%	1%	5%	1%
		Winter pea	-5%	**-2%**	-1%	8%	0%	0%	3%	7%	14%
	EC-EARTH_HIRAM6	Spring pea	-12%	-7%	**-4%**	-2%	-1%	1%	9%	11%	17%
		Winter faba bean	2%	-1%	0%	**8%**	0%	2%	6%	3%	10%
		Winter pea	-5%	-2%	-2%	**10%**	0%	2%	4%	7%	17%
	IPSL_WRF	Spring pea	**-32%**	**-26%**	**-14%**	**-14%**	**-9%**	1%	-9%	-22%	**-36%**
		Winter faba bean	**7%**	-2%	0%	**17%**	-1%	2%	-6%	-6%	-15%
		Winter pea	-11%	**-19%**	**-10%**	8%	**-4%**	2%	**-14%**	-12%	-26%